Molecular Pharmacology Fast Forward. Published on May 14, 2015 as DOI: 10.1124/mol.114.096883
This article has not been copyedited and formatted. The final version may differ from this version.

Synthesis and Evaluation of a Novel Deguelin Derivative, L80, which Disrupts ATP Binding to the C-terminal Domain of Heat Shock Protein 90

Su-Chan Lee, Hye-Young Min, Hoon Choi, Ho Shin Kim, Kyong-Cheol Kim, So-Jung Park, Myeung A Seong, Ji Hae Seo, Hyun-Ju Park, Young-Ger Suh, Kyu-Won Kim, Jeewoo Lee, Ho-Young Lee

College of Pharmacy and Research Institute of Pharmaceutical Sciences, Seoul National University, Seoul 151-742, Republic of Korea (S.C.L., H.Y.M., H.C., H.S.K., K.C.K., M.A.S., J.H.S., Y.G.S., K.W.K., J.L., H.Y.L.)

School of Pharmacy, Sungkyunkwan University, Suwon 440-746, Korea (S.J.P., H.J.P.)

Molecular Pharmacology Fast Forward. Published on May 14, 2015 as DOI: 10.1124/mol.114.096883
This article has not been copyedited and formatted. The final version may differ from this version.

Running title: Blockade of the C-terminal Hsp90 ATP binding domain by L80

Correspondence to:

Ho-Young Lee, Ph.D.

College of Pharmacy and Research Institute of Pharmaceutical Sciences,

Seoul National University,

1 Gwanak-ro, Gwanak-gu, Seoul 151-742, Republic of Korea

Phone: +82-2-880-9277; Fax: +82-2-6280-5327; E-mail: hylee135@snu.ac.kr

Number of text pages: 30

Number of figures: 7

Number of supplemental figures: 10

Number of references: 50

Number of words in Abstract: 231

Number of words in Introduction: 642

Number of words in Discussion: 1512

Abbreviation: HSP90, the 90-kDa molecular chaperone heat shock protein; **NSCLC**, non-small cell lung cancer; **HIF-1α**, hypoxia-inducible factor-1α; **VEGF**, vascular endothelial growth factor; **IGF2**, insulin-like growth factor 2

Molecular Pharmacology Fast Forward. Published on May 14, 2015 as DOI: 10.1124/mol.114.096883
This article has not been copyedited and formatted. The final version may differ from this version.

Abstract

The clinical benefit of current anticancer regimens for lung cancer therapy is still limited due to moderate efficacy, drug resistance, and recurrence. Therefore, the development of effective anticancer drugs for first-line therapy and for optimal second-line treatment is necessary. As the 90-kDa molecular chaperone heat shock protein (Hsp90) contributes to the maturation of numerous mutated or overexpressed oncogenic proteins, targeting Hsp90 may offer an effective anticancer therapy. Here, we investigated antitumor activities and toxicity of a novel deguelin derived C-terminal Hsp90 inhibitor, designated L80. L80 displayed significant inhibitory effects on the vialbility, colony formation, angiogenesis-stimulating activity, migration, and invasion of a panel of non-small cell lung cancer (NSCLC) cell lines and their sublines with acquired resistance to paclitaxel with minimal toxicity to normal lung epithelial cells, hippocampal cells, vascular endothelial cells, and ocular cells. Biochemical analyses and molecular docking simulation revealed that L80 disrupted Hsp90 function by binding to the C-terminal ATP-binding pocket of Hsp90, leading to the disruption of the interaction between hypoxia-inducible factor (HIF)-1α and Hsp90, downregulation of HIF-1α and its target genes, including vascular endothelial growth factor (VEGF) and insulin-like growth factor 2 (IGF2), and decreased the expression of various Hsp90 client proteins. Consistent with these *in vitro* findings, L80 exhibited significant antitumor and antiangiogenic activities in H1299 xenograft tumors. These results suggest that L80 represents a novel C-terminal Hsp90 inhibitor with effective anticancer activities with minimal toxicities.

Molecular Pharmacology Fast Forward. Published on May 14, 2015 as DOI: 10.1124/mol.114.096883
This article has not been copyedited and formatted. The final version may differ from this version.

Introduction

Lung cancer is the leading cause of cancer-related human deaths worldwide. Despite several decades of intense efforts to develop therapeutic interventions, the 5-year survival rate for lung cancer is still less than 20% (Jemal et al., 2011; Siegel et al., 2013). Lung cancer is briefly classified into non-small cell lung cancer (NSCLC) and small-cell lung cancer (SCLC), and about 85-90% of lung cancers are diagnosed as NSCLC. Based on chemotherapy resistance and toxicity, the focus of anticancer drug development has moved to therapies that target specific cellular molecules (Dobbelstein and Moll, 2014). Some therapies have resulted in remarkable tumor reductions in some types of lung cancers (Lee et al., 2013; Sharma et al., 2007); however, many patients do not respond to these drugs, and initially responsive patients ultimately develop resistance after prolonged, continuous treatment. Therefore, the development of novel therapeutic drugs that involve identified molecular mechanisms and promising antitumor activities in both chemotherapy-naïve and resistant cancer cells with suitable therapeutic indices needs to be investigated.

Deguelin, a naturally occurring rotenoid, might be considered as a promising lead compound for the rapid production of structural analogs for lung cancer treatment. In previous studies, we and others have demonstrated that deguelin exhibits profound antiproliferative effects on human premalignant and malignant bronchial epithelial cells and a variety of cancer cells without cytotoxicity to normal cells (Chun et al., 2003; Kang et al., 2012; Lee et al., 2010; Mehta et al., 2013a; Mehta et al., 2013b; Murillo et al., 2009; Suh et al., 2013; Thamilselvan et al., 2011). Furthermore, deguelin has shown *in vivo* effectiveness in suppressing the growth of xenograft tumors and lung tumor formation in tobacco carcinogen-treated A/J mice and in genetically engineered mice with mutant K-Ras (Chun et al., 2003; Kim et al., 2008; Lee et al., 2005; Woo et al., 2009). Structural biology and molecular modeling techniques have revealed that deguelin exhibits antitumor and antiangiogenic activities by targeting heat shock protein 90 (Hsp90), which functions as a

Molecular Pharmacology Fast Forward. Published on May 14, 2015 as DOI: 10.1124/mol.114.096883
This article has not been copyedited and formatted. The final version may differ from this version.

molecular chaperone and is required for the stability and proper function of many oncogenic proteins, including hypoxia inducible factor (HIF)-1α, mutated p53, mitogen-activated protein kinase kinase (MEK1/2), cyclin-dependent kinase 4 (CDK4), erbB2, and Akt (Oh et al., 2008; Oh et al., 2007).

A concern on the use of deguelin as an anticancer drug is its potential toxicities which could be an obstacle to its clinical development. A previous study reported a Parkinson's disease-like syndrome (PDS) in rats treated with deguelin at high doses (Caboni et al., 2004). In addition, it was reported that Hsp90 inhibitors may induce ocular toxicity (Kanamaru et al., 2014). Although it is not clear whether therapeutic doses of deguelin would induce the side effects and whether the side effects can be relieved after drug withdrawal, the potential toxicities of deguelin can be a considerable obstacle to its clinical use. To circumvent these issues, we have investigated to develop deguelin analogs which harbor less or no potential toxicity to various normal cells.

The aim of the current study was to evaluate the antitumor effects and potential toxicity of a novel deguelin analog, designated (6,7-dimethoxyquinolin-4-yl)(5-methoxy-2,2-dimethyl-*2H*-chromen-6-yl)methyl acetate (L80; **Fig. 1A**), and to investigate the mechanisms underlying the anticancer activities of this analog in lung cancer. We found that L80 has significant antitumor and antiangiogenic activities *in vitro* in multiple lines of NSCLC cells and their sublines carrying acquired chemoresistance and *in vivo* in xenograft tumors. L80 was found to possess minimal toxicities to normal lung epithelial cells, hippocampal cells, retinal pigment epithelial cells, and vascular endothelial cells, whereas deguelin induced significant cytotoxicities in these cells. L80 appeared to disrupt Hsp90 function by directly interacting with the C-terminal domain of Hsp90 and the concomitant destabilization of multiple Hsp90 client proteins, including HIF-1α. Collectively, these results suggest the potential use of L80 as a novel C-terminal Hsp90 inhibitor with effective antitumor activity without severe side effects.

Molecular Pharmacology Fast Forward. Published on May 14, 2015 as DOI: 10.1124/mol.114.096883
This article has not been copyedited and formatted. The final version may differ from this version.

Materials and Methods

Detailed experimental procedures are described in the Supplementary Information.

Reagents

Antibodies against cleaved caspase-3, β-tubulin, Akt, and ErbB2 were purchased from Cell Signaling Technology (Danvers, MA, USA). Antibodies against cleaved PARP and HIF-1α were purchased from BD Biosciences (San Jose, CA, USA). Ni-NTA agarose was purchased from Invitrogen (Carlsbad, CA, USA). The first-strand cDNA synthesis kit was purchased from Dakara Korea Biomedical, Inc. (Seoul, Republic of Korea). The Econotaq DNA polymerase was purchased from Lucigen Corp. (Middleton, WI, USA). 3-(4,5-Dimethylthiazol-2-yl)-2,5-diphenyltetrazolium bromide (MTT), propidium iodide (PI), crystal violet, and other chemicals were purchased from Sigma-Aldrich (St. Louis, MO, USA) unless otherwise specified.

Cell culture

H1299, A549, and BEAS-2B cells were purchased from the American Type Culture Collection (ATCC, Manassas, VA, USA). Human bronchial epithelial cells (HBECs) were kindly provided by Dr. John Minna (The University of Texas Southwestern Medical Center, Dallas, TX, USA). HUVECs were purchased from Invitrogen. H226B cells were kindly provided by Dr. Jack A. Roth (The University of Texas M. D. Anderson Cancer Center, Houston, TX, USA). H460/R and H226B/R cells were generated by continuous exposure to increasing concentrations of paclitaxel for more than 6 months.[1] All cell lines were authenticated and validated. NSCLC cells were cultured in RPMI 1640 medium supplemented with 10% fetal bovine serum (FBS) and antibiotics. BEAS-2B and HBEC1

[1] Manuscript in preparation

Molecular Pharmacology Fast Forward. Published on May 14, 2015 as DOI: 10.1124/mol.114.096883
This article has not been copyedited and formatted. The final version may differ from this version.

cells were maintained in K-SFM (Invitrogen) supplemented with EGF and bovine pituitary extracts. Cells were incubated at 37°C with 5% CO_2 in a humidified atmosphere. These cell lines were authenticated by Genetic Resources Core Facility of Johns Hopkins University or by the Korean Cell Line Bank using AmplFLSTR identifiler PCR Amplification kit (Applied Biosystems, Foster, CA, USA; cat. No. 4322288).

MTT assay

To evaluate the effect of L80 on the proliferation of lung cancer cells, MTT assays were performed as described previously (Chang et al., 2012; Oh et al., 2007). Cells (1-2 x 10^3 cells/well in 96-well plates) were treated with increasing concentrations of L80 for 3 days. The drug-containing medium was replaced at 2 days after drug treatment. Cells were treated with MTT (final concentration of 200 μg/ml) and incubated for 2-4 hours at 37°C. The formazan products were dissolved in DMSO, and the absorbance was measured at 570 nm. The data are presented as a percentage of the control group.

Immunoprecipitation and pull-down assay

Immunoprecipitation, the purification of Hsp90 proteins, and a pull-down assay to determine the competitive binding to the ATP-binding pocket using ATP-agarose (Innova Biosciences, Babraham, Cambridge, United Kingdom) were performed according to our previous report (Oh et al., 2007).

Animal studies

All animal procedures were performed using a protocol approved by the Seoul National University Institutional Animal Care and Use Committee (approval No. SNU-130820-6), which was in line with the NIH guideline. For xenograft experiments, H1299 cells (4 x 10^6 cells/mouse) were subcutaneously injected into the right flank of a 6-week old NOD/SCID mouse. After the tumor volume reached 50-150 mm^3, mice were randomly

Molecular Pharmacology Fast Forward. Published on May 14, 2015 as DOI: 10.1124/mol.114.096883
This article has not been copyedited and formatted. The final version may differ from this version.

grouped and treated with vehicle (10% DMSO in corn oil) or L80 (20 mg/kg) six times per week for 3 weeks by intraperitoneal injection. Tumor growth was determined by measuring the short and long diameters of the tumor with a caliper, and body weight was measured twice per week to monitor toxicity. The tumor volume was calculated using the following formula: tumor volume (mm^3) = $(\text{short diameter})^2 \times (\text{long diameter}) \times 0.5$.

Immunohistochemistry

Immunohistochemical analysis to detect CD31 and cleaved caspase-3 expression in the tumors were performed as described previously (Oh et al., 2007).

Statistics

Data are presented as the mean ± SD. The results not included in the main figures are shown in Supplementary Figures. The statistical significance was determined using either two-sided Student's *t*-test or one-way analysis of variance (ANOVA) followed by Dunnett's post hoc test using GraphPad Prism 6 (GraphPad Software Inc., La Jolla, CA, USA). A *P* value less than 0.05 was considered to be statistically significant.

Results

Synthesis of L80

As mentioned previously, we have synthesized a series of structural deguelin analogs to develop lead compounds with enhanced efficacy and/or reduced toxicity compared to deguelin (Chang et al., 2012; Kim et al., 2008). A detailed scheme and the L80 synthesis procedure are described in the Supplemental information. L80 has a dimethoxy quinoline ring and a 1,2-unsaturated benzopyran ring linked by one carbon with an acetyl group. 4-Hydroxy quinolone (compound **2**) was synthesized from 2'-amino-4',5'-dimethoxyacetophenone (compound **1**) through cyclization. The hydroxyl group was

Molecular Pharmacology Fast Forward. Published on May 14, 2015 as DOI: 10.1124/mol.114.096883
This article has not been copyedited and formatted. The final version may differ from this version.

converted to a bromo group by treatment with PBr_3 to give compound **3.** Brominated compound **3** was coupled with an aldehyde (compound **4**) to obtain the desired hydroxyl compound **5**. The aldehyde compound **4** was synthesized from 2,4-dihydroxybenzaldehyde (compound **7**) and 3-methylbut-2-enal through regioselective cyclization and continuous methylation by Jacob's procedure. Finally, compound **6** (L80) (**Fig. 1A**) was formed by the acetylation of compound **5**.

L80 exhibited markedly reduced toxicity to normal cells compared to deguelin

Previous research reported that high concentrations of deguelin can induce behavioral disorder similar to Parkinson's disease-like syndrome (PDS) in rats treated with deguelin at high doses (Caboni et al., 2004), we first assessed the possible permeation of L80 and deguelin through the blood-brain-barrier (BBB) by performing the parallel artificial membrane permeability assay (PAMPA) (Kansy et al., 1998). The PAMPA permits the fast determination of artificial membrane permeation properties of small molecules by passive diffusion (Kansy et al., 1998) Each compound can be classified as either permeable (CNS+; $-\log P_e < 5.4$) or impermeable (CNS−; $-\log P_e > 5.7$) (Di et al., 2003). The $-\log P_e$ for deguelin and L80 were 4.78 (±0.20), and 4.82 (±0.25), respectively (**Figs. 1B, S1A and Table S1**), suggesting that the two drugs may be BBB permeable. We then tested the effects of L80 and deguelin on viability of hippocampal cell line, HT-22. Treatment with deguelin showed significant cytototoxicity in HT-22 cells in a concentration-dependent manner (**Figs.1C and S1B**). In contrast, L80 displayed no obvious inhibitory effects on the viability of HT22 cells even at the highest concentration of 10 μM. These data suggest that, although both deguelin and L80 could be permeable to BBB, L80 may be less toxic to the CNS compared to its mother compound deguelin. We further tested the potential cytotoxicity of L80 and deguelin on normal lung epithelial, retinal pigment epithelial and vascular endothelial cells. To this end, immortalized human bronchial epithelial cell lines (HBEC and BEAS-2B), retinal pigment epithelial cells (RPE), and human umbilical endothelial cells

Molecular Pharmacology Fast Forward. Published on May 14, 2015 as DOI: 10.1124/mol.114.096883
This article has not been copyedited and formatted. The final version may differ from this version.

(HUVECs) were incubated with L80 or deguelin. More than 80% of HBE cells were viable after treatment with 10 μM L80 (**Figs. 1D and S1C**). In contrast, deguelin treatment even at 1 μM showed significant decrease in lung epithelial cell lines. Similarly, cytotoxic effects of L80 on vascular endothelial and retinal epithelial cells were less compared to deguelin (**Figs. 1E, S1D, and S1E**). These overall data indicate markedly reduced cytotoxicity of L80 to normal cells compared to deguelin.

L80 functions as a potent inhibitor of NSCLC cell proliferation and anchorage-dependent and anchorage-independent colony formation

In a previous study, we demonstrated that deguelin inhibits the growth of and induces apoptosis in NSCLC cell lines, with minimum effects on normal human bronchial epithelial cells (HBEs) at *in vitro* concertrations that are attainable *in vivo* (Lee et al., 2004). Hence, we first examined the effects of L80 on viability of NSCLC cell lines (i.e., H1299, A549, H460, and H226B). Because resistance to traditional chemotherapeutic agents is an obstacle to anticancer therapies, we also included NSCLC cell sublines (i.e., H226B/R, H460/R) with acquired resistance against paclitaxel after prolonged exposure. These cell lines were treated with 10^{-7} to 10^{-5} M L80 for 3 days; then, cell viability was measured by the MTT assay. As shown in **Figs. 2A and S2A**, L80 significantly inhibited viability of human NSCLC cells. The inhibitory effect of L80 on the drug-resistant sublines (H460/R and H226B/R) was comparable with that on the corresponding parental cells (H460 and H226B), suggesting that L80 might be applicable to both naïve and chemo-resistant lung cancer cells (**Figs. 2A, 2B, and S1A**). We next examined the effects of L80 on the anchorage-dependent colony forming abilities of the NSCLC cells. As illustrated in **Fig. 2C and S2B,** all tested NSCLC cells showed significantly decreased colony formation after 0.1 to 10 μM of L80 treatment. Because tumorigenic cells can often grow in semisolid media, such as soft agar (Hanahan and Weinberg, 2000), we further tested the effects of L80 on colony formation of NSCLC cells using a semisolid culture condition. Consistent with the cells grown in monolayer culture

Molecular Pharmacology Fast Forward. Published on May 14, 2015 as DOI: 10.1124/mol.114.096883
This article has not been copyedited and formatted. The final version may differ from this version.

conditions, L80 strongly suppressed the indicated NSCLC cell growth in soft agar (**Fig. 2D and S2C**). Notably, H460/R and H226B/R cells formed significantly fewer colonies in soft agar than their corresponding parental cells after treatment with 10 μM L80, suggesting that L80 might deregulate cellular events that regulate anchorage-independent colony forming abilities of NSCLC cells carrying acquired paclitaxel resistance. These results suggest that L80 effectively inhibits survival, and the colony-forming abilities of both naïve and chemo-resistant NSCLC cells with minimal toxicity to normal HBECs.

L80 induces apoptotic cell death in NSCLC cells

To investigate the mechanisms by which L80 inhibited cancer cell proliferation and colony formation, the effect of L80 on cell cycle progression was examined by flow cytometry. Treatment with 10 μM L80 induced an accumulation of 20.8% of H1299 cells, 18.6% of H460 cells, 9% of H226 cells, 11.3% of H226B/R cells, and 20.8% of H460/R cells in the sub-G0/G1 phase, suggesting that it has proapoptotic activity in NSCLC cells (**Figs. 3A and S3A**). L80-induced apoptosis was further further supported by Western blot analysis showing the concentration-dependent increase in poly-(ADP-ribose) polymerase (PARP) cleavage (**Fig. 3B**). These results indicate that the antiproliferative activities of L80 in NSCLC cells are at least in part due to increased apoptosis.

L80 suppresses HIF-1α expression and angiogenic activities in NSCLC cells

Based on the previous findings regarding the antiangiogenic activity of deguelin through suppression of HIF-1α (Oh et al., 2008; Oh et al., 2007), we tested the effect of L80 on HIF-1α expression and its target genes, including VEGF and IGF2. Treatment with L80 under hypoxic conditions suppressed the expression of HIF-1α in a concentration-dependent manner (**Figs. 4A and S4A**) and significantly downregulated hypoxia response element (HRE)-dependent reporter activity (**Figs. 4B and S4B**). Consistent with these results, the VEGF and IGF2 mRNA and protein expression levels were markedly decreased in L80-

Molecular Pharmacology Fast Forward. Published on May 14, 2015 as DOI: 10.1124/mol.114.096883
This article has not been copyedited and formatted. The final version may differ from this version.

treated NSCLC cells (**Figs. 4C and S4C**), indicating that the L-80-mediated decrease in HIF-1α transcriptional activity led to a downregulation of VEGF expression. The inhibitory effect of L80 on VEGF expression was comparable with that of deguelin (**Figs. 4D and S4D**). Because tumor angiogenesis is stimulated by angiogenic factors secreted from cancer cells, we analyzed whether L80 could inhibit the angiogenesis-stimulating activities of NSCLC cells. Thus, we assessed the effects of CM collected from L80-treated H1299 cells on HUVECs. We observed that treatment with CM from L80-treated H1299 cells induced significantly decreased HUVEC tube formation compared with CM from vehicle-treated cells (**Figs. 4E and S4E**)**.** These findings suggest that L80 possesses the ability to suppress tumor angiogenesis by inhibiting HIF-1α expression.

L80 decreases migration and invasion of NSCLC cells

Deguelin suppresses the migration and invasion of various types of cancer cells, including pancreatic and prostate cancer cells (Boreddy and Srivastava, 2013; Thamilselvan et al., 2011). Hence, we examined the effects of L80 on NSCLC cell migration and the invasion of NSCLC cells by performing *in vitro* migration and invasion assays. We observed that pretreatment with 10 μM L80 for 24 h, which showed no detectable effect on cell proliferation (**Figs. 5A and S5A**), had consistent inhibitory effects on the migration (**Figs. 5B and S5B**) and invasion (**Figs. 5C and S5C**) of H1299, H226B, and H226B/R cells. These findings suggest that L80 might regulate cellular events involved in the migration and invasion of NSCLC cells and their sublines with acquired paclitaxel resistance.

Effects of L80 on tumor growth and CD31 expression

We further evaluated the antitumor activities of L80 in H1299 xenograft tumors established in NOD/SCID mice. Mice bearing tumors (with volumes of 50-150 mm^3) were randomly grouped and received L80 (20 mg/kg body weight) for 3 weeks. L80 significantly suppressed the growth of H1299 xenograft tumors (**Fig. 6A**). During the treatment, the body

Molecular Pharmacology Fast Forward. Published on May 14, 2015 as DOI: 10.1124/mol.114.096883
This article has not been copyedited and formatted. The final version may differ from this version.

weight of mice did not significantly change between the control and L80-treated groups, suggesting minimal toxicity of L80 to the mice (**Fig. S6**). Consistent with notable antitumor effects, the tumoral expression of cleaved caspase-3, an indicator of apoptotic cell death, was markedly increased in L80-treated tumors (**Fig. 6B**). The expression of CD31 was decreased in tumors treated with L80, suggesting antiangiogenic effects of L80 (**Fig. 6C**). These results suggest that L80 displays effective antitumor activities in NSCLC xenograft tumors by inhibiting tumor angiogenesis and by inducing apoptosis.

L80 inhibits Hsp90 function by binding to the ATP-binding pocket in the C-terminal domain of Hsp90

We investigated the mechanism by which L80 suppressed the antumor activities of NSCLC cells. Based on our previous results showing that deguelin blocks Hsp90 function by directly binding to the ATP-binding pocket of Hsp90, resulting in the degradation of various client proteins, including HIF-1α (Isaacs et al., 2002; Oh et al., 2007), we assessed whether Hsp90 was involved in L80-mediated anticancer activity. We first performed co-immunoprecipitation assays to examine the effect of L80 on the Hsp90 and HIF-1α interaction in H1299 cells. We observed a strong physical interaction between HIF-1α and Hsp90 in H1299 cells. However, this interaction was strongly diminished in the cells pretreated with L80 for 1 h, when HIF-1α and Hsp90 protein expression levels were not affected (**Figs. 7A and S7A**). We further confirmed this finding by performing a pull-down assay. H1299 lysates were incubated with recombinant proteins containing the HLH–PAS–ODD domain of HIF-1α, which is essential for complex formation with Hsp90 and has a sensitivity to Hsp90 inhibitors (Katschinski et al., 2004; Minet et al., 1999), in the presence or absence of L80. The level of Hsp90 bound to the recombinant HIF-1α was determined by Western blot analysis. As shown in **Figs. 7B and S7B**, the interaction between Hsp90 and HIF-1α was markedly diminished by L80 treatment. The suppression of Hsp90 function was further confirmed by assessing the effect of L80 on the expression of other Hsp90 client

Molecular Pharmacology Fast Forward. Published on May 14, 2015 as DOI: 10.1124/mol.114.096883
This article has not been copyedited and formatted. The final version may differ from this version.

proteins. As shown in **Figs. 7C and S7C**, treatment with L80 effectively inhibited the expression of Hsp90 client proteins, including ErbB2 and Akt, in a concentration-dependent manner. Thus, these results suggest that L80 can directly modulate the function of Hsp90.

In general, Hsp90 inhibitors interfere with the binding of ATP to the nucleotide-binding pocket of Hsp90 in the N- or C-terminal domains (Whitesell and Lindquist, 2005). The nucleotide-binding pocket in the N-terminal domain was first identified and is the predominant ATP-binding site in Hsp90. ATP can bind to an additional binding pocket in the C-terminal domain of Hsp90 when the N-terminal binding sites are occupied (Soti et al., 2002; Whitesell and Lindquist, 2005). We investigated whether L80 binds to the ATP-binding pocket of Hsp90, and if so, whether it was the N- or the C-terminal pocket. Thus, we prepared recombinant Hsp90 proteins containing full length (FL) protein, the N-terminal and middle (NM) domain, the middle (M) domain, and the C-terminal (C) domain. The binding of each HSP90 domain to ATP-agarose was examined in the presence of L80. We observed a complete disruption of the interaction between ATP-agarose and the C domain of Hsp90 in the presence of L80 (1 μM), while the same concentration of L80 showed a partial or no effect on ATP binding to the FL protein or the NM domain, respectively (**Fig. 7D and S7D**). These results suggest that L80 is able to bind to the C-terminal ATP-binding pocket of Hsp90 and thus hamper Hsp90 function.

We further conducted a computational molecular modeling to ensure the binding of L80 to the C-terminal ATP-binding pocket of Hsp90. We carried out docking study of ATP and L80 in the C-terminal ATP-binding pocket of hHsp90 homodimer. The active site was determined based on reported hHsp90 C-terminal ATP-binding site (Sgobba et al., 2008). As shown in **Fig. 7E**, active site is located at the dimerization interface. After docking, we compared docking pose and score of ATP with those of L80. As illustrated in **Fig. 7F**, ATP (white carbon) fits well into the ATP-binding pocket of chain A. The adenine ring occupies deep into the hydrophobic pocket. The phosphate moiety interacts with multiple hydrogen bonds with Glu611, and 3′-hydroxy of sugar moiety forms an additional hydrogen bond with

Molecular Pharmacology Fast Forward. Published on May 14, 2015 as DOI: 10.1124/mol.114.096883
This article has not been copyedited and formatted. The final version may differ from this version.

Ser677 in chain A. Although L80 is partially overlaid over sugar-phosphate moiety of ATP, L80 binds at the center of interface between chain A and B with higher docking score ($-\log K_d$ = 7.13) than ATP ($-\log K_d$ = 6.29) (**Fig. 7G**). Two oxygen atoms of acetoxy group form the a hydrogen bond with an amide at Lys 615 in chain A and the oxygen atom of methoxy group also forms a hydrogen bond with a hydrogen bond at Ser677 which is a part of ATP-binding pocket in chain B. A full image of Hsp90:L80 complex (**Fig. 7E**) reveals that L80 occupies in the middle of active site located at the interface of C-terminal homodimer. Taken together, our docking results suggests that L80 can bind to the C-terminal ATP binding site competitively with ATP, leading to stabilize the open state of Hsp90 homodimer by interacting with both A and B chain.

Discussion

The aim of the current study was to determine the toxicity, efficacy and action mechanisms of a deguelin-derived analog, designated L80, for potential clinical use. The data presented show that the proliferative, angiogenic, and metastatic activities of NSCLC cells and their sublines with acquired chemoresistance were significantly inhibited by L80. L80 also exhibited significant antitumor activity *in vivo* in H1299 NSCLC xenograft tumors, which was accompanied by increased apoptosis and decreased vascular formation. Mechanistically, L80 effectively disrupted Hsp90 function by directly binding to the C-terminal ATP-binding pocket of Hsp90, leading to the reduced expression of Hsp90 client proteins, including HIF-1α. These data suggest that L80 may have potential as an anticancer drug targeting Hsp90 through mechanisms that are different than those targeted by the well-known N-terminal Hsp90 inhibitors.

Hsp90, which belongs to a family of ATPase-containing molecular chaperones, functions to prevent its client proteins from misfolding upon heat shock or other stresses, thereby promoting their stabilization (Trepel et al., 2010; Whitesell and Lindquist, 2005). Cancer cells are normally in a state of proteotoxic pressure due, in part, to the accumulation

Molecular Pharmacology Fast Forward. Published on May 14, 2015 as DOI: 10.1124/mol.114.096883
This article has not been copyedited and formatted. The final version may differ from this version.

of mutated molecules that could lead to cell lethality (Bagatell and Whitesell, 2004). Numerous Hsp90 client proteins, such as those in the epidermal growth factor receptor (EGFR) family, c-Met, Akt, Src, and B-Raf, are often mutated or overexpressed in several types of human cancer, including NSCLC (Shimamura and Shapiro, 2008; Whitesell and Lindquist, 2005), most likely to compensate for the insult. These oncogenic kinases mediate cancer cell proliferation, survival, angiogenesis, invasion, and metastasis, all of which play critical roles in cancer progression and resistance to conventional or targeted anticancer agents, including paclitaxel, cisplatin, erlotinib, and trastuzumab (Bao et al., 2009; Sawai et al., 2008; Solar et al., 2007; Trepel et al., 2010; Wainberg et al., 2013; Whitesell and Lindquist, 2005). Therefore, targeting Hsp90 would be an effective way for treating cancer and overcoming anticancer drug resistance, and it is a promising target for anticancer drug design. Consistent with this hypothesis, a growing body of evidence has shown the importance of an Hsp90 inhibitor for the treatment of cancer. Inhibition of Hsp90 induces the simultaneous degradation of numerous oncogenic Hsp90 client proteins, leading to an effective antitumor outcome (Trepel et al., 2010; Whitesell and Lindquist, 2005). The Hsp90 inhibitor ganetespib, alone or in combination with other anticancer drugs, displays effective antitumor effects in lung cancer cells, especially lung cancer harboring mutant K-Ras (Acquaviva et al., 2012). Another Hsp90 inhibitor, NVP-AUY922, has also shown potent antiproliferative and antitumor effects in various lung cancer cells (Garon et al., 2013).

Although several clinical trials to evaluate the effectiveness of Hsp90 inhibitors in lung cancer treatment are ongoing (Jhaveri et al., 2012), the main drawbacks of Hsp90 inhibitors are undesirable side effects, poor water solubility, and toxicity (Trepel et al., 2010). Therefore, it is necessary to develop novel strategies to target Hsp90. Zhang et al. suggested a novel strategy for Hsp90 inhibition through the disruption of Hsp90-co-chaperone interactions (Zhang et al., 2008). Another strategy targeting the C-terminal ATP-binding pocket of Hsp90 has been proposed because the antibiotic novobiocin binds with low affinity to a C-terminal ATP-binding pocket (Marcu et al., 2000a; Marcu et al., 2000b). Recently, more potent

Molecular Pharmacology Fast Forward. Published on May 14, 2015 as DOI: 10.1124/mol.114.096883
This article has not been copyedited and formatted. The final version may differ from this version.

analogs of novobiocin have been developed (Burlison et al., 2008; Burlison et al., 2006). Although the antitumor activities of these analogs need to be evaluated in relevant *in vivo* models of human cancer, such new approaches could provide a novel opportunity for Hsp90 inhibition.

We previously reported that deguelin, a natural product that competes with ATP on the Hsp90 ATP-binding pocket, leading to decreases in many Hsp90 client oncoproteins without detectable toxicities to normal lung epithelial cells *in vitro* and to major organs in mouse tissues *in vivo*, has potential as an anticancer drug (Oh et al., 2007). However, the potential neuronal toxicity of deguelin, which most likely occurs through the inhibition of NADH dehydrogenase (Caboni et al., 2004), raises concern for its use in human cancer patients. Hence, we have attempted to develop deguelin derivatives as lead compounds for the development of novel Hsp90 inhibitors (Chang et al., 2012; Kim et al., 2008; Oh et al., 2007). In our structure-activity relationship (SAR) studies, the 2,2-dimethyl-2*H*-chromene moiety of deguelin seemed to be responsible for occupying the ATP-binding pocket of Hsp90 *via* hydrophobic interactions. In addition, two dimethyoxy groups at the C9 and C10 positions, the terminal methoxy group in the 2,2-dimethyl-2*H*-chromene moiety, and a hydrogen bond donor group at the C7 position seemed to be important for the antiproliferative activity (Chang et al., 2012; Oh et al., 2007). In recent studies, we and others reported inhibitory effects of a compound containing 2,2-dimethyl-2*H*-chromene moiety on HIF-1α expression (Chang et al., 2012; Tan et al., 2005). In the current study, we show that L80, which shares these critical moieties of the deguelin, has antiangiogenic and antitumor activities.

We found several features of L80 that make the analog a lead compound for the development of novel anticancer drugs. First, L80 appeared to retain the potent antiproliferative and apoptotic activities of its mother compound *in vitro* and *in vivo* with minimal toxicity to normal lung epithelial, hippocampal, retinal pigment epithelial, and vascular endothelial cells. Tissue samples taken from several organs, including liver, of L80-treated mice revealed no pathohistological changes. This finding is important because the

Molecular Pharmacology Fast Forward. Published on May 14, 2015 as DOI: 10.1124/mol.114.096883
This article has not been copyedited and formatted. The final version may differ from this version.

main hurdle for the currently available Hsp90 inhibitors in clinical trials is liver and ocular toxicities (Jhaveri et al., 2012). Second, L80 effectively suppressed NSCLC cells' activities for angiogenesis stimulation, migration, and invasion. This finding is significant because the majority of cancer patients die from metastatic disease; effective therapeutic drugs would be expected not only to lower primary tumor burden but also to interrupt the metastatic cascade. Third, L80 seemed to inhibit Hsp90 function through mechanisms that are different than those regulated by the currently available Hsp90 inhibitors. We found that the blockade of Hsp90 interaction with HIF-1α and the destabilizing of Hsp90 client proteins including HIF-1α by L80 treatment were associated with decreased binding of ATP-agarose to the C-terminal domain of the Hsp90 protein. Considering the role of C-terminal dimerization during Hsp90 conformational cycle and the inverse correlation between N- and C-terminal dimerization (Ratzke et al., 2010; Soti et al., 2002), binding of L80 to the C-terminal Hsp90 homodimer may cause stabilization of open conformation of Hsp90, resulting in prohibiting global conformational changes of Hsp90 such as N-terminal dimerization and the formation of ATP binding pocket. The computational analysis using molecular docking modeling suggests that L80 can bind to the C-terminal ATP binding site competitively with ATP L80 and lead the stabilization of open form of Hsp90 homodimer, further confirming the inhibitory effect of L80 on Hsp90 function by binding to the C-terminal ATP binding pocket of Hsp90. These findings suggests that L80 can serve as a functional inhibitor of Hsp90 that blocks ATP binding to the C-terminal binding pocket of Hsp90. Because the dimerization of Hsp90 mediated by the C-terminal is critical for its chaperone function and because the ATP-binding pocket at the C-terminal is necessary for the close association between two N-terminals in the ATP-bound state (Wainberg et al., 2013), targeting the C-terminal domain of Hsp90 could be an alternative and effective allosteric approach to functionally inhibiting Hsp90. Although additional studies are required to explore the detailed mechanisms by which L80 interacts with the ATP-binding pocket in the C-terminal of Hsp90, the mode of action of L80 makes it a leading chemical for the development of novel Hsp90 inhibitors. Fourth, L80 did not

Molecular Pharmacology Fast Forward. Published on May 14, 2015 as DOI: 10.1124/mol.114.096883
This article has not been copyedited and formatted. The final version may differ from this version.

discriminate naïve NSCLC cells from those with acquired resistance to paclitaxel. Previous studies have suggested that Hsp90 is involved in anticancer drug resistance and that treatment with an Hsp90 inhibitor overcomes the resistance to conventional or molecular-targeted anticancer drugs (Bao et al., 2009; Sawai et al., 2008; Solar et al., 2007; Wainberg et al., 2013), emphasizing the importance of Hsp90 inhibition to overcome anticancer drug resistance. Although additional *in vitro* and *in vivo* studies are required to evaluate the effectiveness of L80, either alone or in combination with paclitaxel, our results suggest that the suppression of Hsp90 function may overcome resistance to paclitaxel, which is frequently used for the treatment of patients with NSCLC (Ramalingam and Belani, 2004). Although the mechanisms mediating the different affinities of L80 to the C- and N-terminal ATP-binding pockets of Hsp90 have not been fully elucidated, these potent *in vitro* and *in vivo* antitumor activities of L80 in NSCLC cells support the potential of L80 as a candidate for the development of anticancer agents.

In summary, the present study suggests that L80 displays significant antitumor activities in NSCLC by binding to the ATP-binding pocket in the C-terminal of Hsp90, thus disrupting Hsp90 function. Overall, the data presented provide compelling evidence for the continued development of L80-based C-terminal Hsp90 inhibitor as promising alternatives to the currently available N-terminal inhibitors for the treatment of human malignancies, including NSCLC. These results suggest that L80 may be a novel Hsp90 inhibitor with effective antitumor effect on NSCLC. Further studies are warranted to investigate the effectiveness of L80 in additional preclinical and clinical settings.

Molecular Pharmacology Fast Forward. Published on May 14, 2015 as DOI: 10.1124/mol.114.096883
This article has not been copyedited and formatted. The final version may differ from this version.

Authorship contribution

Participated in research design: Su-Chan Lee and Ho-Young Lee

Conducted experiments: Su-Chan Lee, Hoon Choi, Myeung A Seong, So-Jung Park and Ji Hae Seo

Contributed new reagents or analytic tools: Ho Shin Kim, Kyong-Cheol Kim, and Jeewoo Lee, Young-Ger Suh, Hyun-Ju Park, Kyu-Won Kim

Performed data analysis: Su-Chan Lee and Ho-Young Lee

Wrote or contributed to the writing of the manuscript: Hye-Young Min and Ho-Young Lee

Molecular Pharmacology Fast Forward. Published on May 14, 2015 as DOI: 10.1124/mol.114.096883
This article has not been copyedited and formatted. The final version may differ from this version.

References

Acquaviva J, Smith DL, Sang J, Friedland JC, He S, Sequeira M, Zhang C, Wada Y and Proia DA (2012) Targeting KRAS-mutant non-small cell lung cancer with the Hsp90 inhibitor ganetespib. *Molecular cancer therapeutics* **11**(12): 2633-2643.

Bagatell R and Whitesell L (2004) Altered Hsp90 function in cancer: a unique therapeutic opportunity. *Molecular cancer therapeutics* **3**(8): 1021-1030.

Bao R, Lai CJ, Wang DG, Qu H, Yin L, Zifcak B, Tao X, Wang J, Atoyan R, Samson M, Forrester J, Xu GX, DellaRocca S, Borek M, Zhai HX, Cai X and Qian C (2009) Targeting heat shock protein 90 with CUDC-305 overcomes erlotinib resistance in non-small cell lung cancer. *Molecular cancer therapeutics* **8**(12): 3296-3306.

Boreddy SR and Srivastava SK (2013) Deguelin suppresses pancreatic tumor growth and metastasis by inhibiting epithelial-to-mesenchymal transition in an orthotopic model. *Oncogene* **32**(34): 3980-3991.

Burlison JA, Avila C, Vielhauer G, Lubbers DJ, Holzbeierlein J and Blagg BS (2008) Development of novobiocin analogues that manifest anti-proliferative activity against several cancer cell lines. *The Journal of organic chemistry* **73**(6): 2130-2137.

Burlison JA, Neckers L, Smith AB, Maxwell A and Blagg BS (2006) Novobiocin: redesigning a DNA gyrase inhibitor for selective inhibition of hsp90. *Journal of the American Chemical Society* **128**(48): 15529-15536.

Caboni P, Sherer TB, Zhang N, Taylor G, Na HM, Greenamyre JT and Casida JE (2004) Rotenone, deguelin, their metabolites, and the rat model of Parkinson's disease. *Chemical research in toxicology* **17**(11): 1540-1548.

Chang DJ, An H, Kim KS, Kim HH, Jung J, Lee JM, Kim NJ, Han YT, Yun H, Lee S, Lee G, Lee S, Lee JS, Cha JH, Park JH, Park JW, Lee SC, Kim SG, Kim JH, Lee HY, Kim KW and Suh YG (2012) Design, synthesis, and biological evaluation of novel deguelin-based heat shock protein 90 (HSP90) inhibitors targeting proliferation and angiogenesis. *Journal of medicinal chemistry* **55**(24): 10863-10884.

Chun KH, Kosmeder JW, 2nd, Sun S, Pezzuto JM, Lotan R, Hong WK and Lee HY (2003) Effects of deguelin on the phosphatidylinositol 3-kinase/Akt pathway and apoptosis in premalignant human bronchial epithelial cells. *Journal of the National Cancer Institute* **95**(4): 291-302.

Di L, Kerns EH, Fan K, McConnell OJ and Carter GT (2003) High throughput artificial membrane permeability assay for blood-brain barrier. *European journal of medicinal chemistry* **38**(3): 223-232.

Dobbelstein M and Moll U (2014) Targeting tumour-supportive cellular machineries in anticancer drug development. *Nature reviews Drug discovery* **13**(3): 179-196.

Garon EB, Finn RS, Hamidi H, Dering J, Pitts S, Kamranpour N, Desai AJ, Hosmer W, Ide S, Avsar E, Jensen MR, Quadt C, Liu M, Dubinett SM and Slamon DJ (2013) The HSP90 inhibitor NVP-AUY922 potently inhibits non-small cell lung cancer growth. *Molecular cancer therapeutics* **12**(6): 890-900.

Hanahan D and Weinberg RA (2000) The hallmarks of cancer. *Cell* **100**(1): 57-70.

Isaacs JS, Jung YJ, Mimnaugh EG, Martinez A, Cuttitta F and Neckers LM (2002) Hsp90 regulates a von Hippel Lindau-independent hypoxia-inducible factor-1 alpha-degradative pathway. *The Journal of biological chemistry* **277**(33): 29936-29944.

Jemal A, Bray F, Center MM, Ferlay J, Ward E and Forman D (2011) Global cancer statistics. *CA: a cancer journal for clinicians* **61**(2): 69-90.

Jhaveri K, Taldone T, Modi S and Chiosis G (2012) Advances in the clinical development of heat shock protein 90 (Hsp90) inhibitors in cancers. *Biochimica et biophysica acta* **1823**(3): 742-755.

Kanamaru C, Yamada Y, Hayashi S, Matsushita T, Suda A, Nagayasu M, Kimura K and Chiba S (2014) Retinal toxicity induced by small-molecule Hsp90 inhibitors in beagle dogs. *The Journal of toxicological sciences* **39**(1): 59-69.

Kang HW, Kim JM, Cha MY, Jung HC, Song IS and Kim JS (2012) Deguelin, an Akt inhibitor, down-regulates NF-kappaB signaling and induces apoptosis in colon cancer cells and

inhibits tumor growth in mice. *Digestive diseases and sciences* **57**(11): 2873-2882.

Kansy M, Senner F and Gubernator K (1998) Physicochemical high throughput screening: parallel artificial membrane permeation assay in the description of passive absorption processes. *Journal of medicinal chemistry* **41**(7): 1007-1010.

Katschinski DM, Le L, Schindler SG, Thomas T, Voss AK and Wenger RH (2004) Interaction of the PAS B domain with HSP90 accelerates hypoxia-inducible factor-1alpha stabilization. *Cellular physiology and biochemistry : international journal of experimental cellular physiology, biochemistry, and pharmacology* **14**(4-6): 351-360.

Kim WY, Chang DJ, Hennessy B, Kang HJ, Yoo J, Han SH, Kim YS, Park HJ, Seo SY, Mills G, Kim KW, Hong WK, Suh YG and Lee HY (2008) A novel derivative of the natural agent deguelin for cancer chemoprevention and therapy. *Cancer prevention research* **1**(7): 577-587.

Lee CK, Brown C, Gralla RJ, Hirsh V, Thongprasert S, Tsai CM, Tan EH, Ho JC, Chu da T, Zaatar A, Osorio Sanchez JA, Vu VV, Au JS, Inoue A, Lee SM, Gebski V and Yang JC (2013) Impact of EGFR inhibitor in non-small cell lung cancer on progression-free and overall survival: a meta-analysis. *Journal of the National Cancer Institute* **105**(9): 595-605.

Lee H, Lee JH, Jung KH and Hong SS (2010) Deguelin promotes apoptosis and inhibits angiogenesis of gastric cancer. *Oncology reports* **24**(4): 957-963.

Lee HY, Oh SH, Woo JK, Kim WY, Van Pelt CS, Price RE, Cody D, Tran H, Pezzuto JM, Moriarty RM and Hong WK (2005) Chemopreventive effects of deguelin, a novel Akt inhibitor, on tobacco-induced lung tumorigenesis. *Journal of the National Cancer Institute* **97**(22): 1695-1699.

Lee HY, Suh YA, Kosmeder JW, Pezzuto JM, Hong WK and Kurie JM (2004) Deguelin-induced inhibition of cyclooxygenase-2 expression in human bronchial epithelial cells. *Clinical cancer research : an official journal of the American Association for Cancer Research* **10**(3): 1074-1079.

Marcu MG, Chadli A, Bouhouche I, Catelli M and Neckers LM (2000a) The heat shock protein 90 antagonist novobiocin interacts with a previously unrecognized ATP-binding domain in the carboxyl terminus of the chaperone. *The Journal of biological chemistry* **275**(47): 37181-37186.

Marcu MG, Schulte TW and Neckers L (2000b) Novobiocin and related coumarins and depletion of heat shock protein 90-dependent signaling proteins. *Journal of the National Cancer Institute* **92**(3): 242-248.

Mehta R, Katta H, Alimirah F, Patel R, Murillo G, Peng X, Muzzio M and Mehta RG (2013a) Deguelin action involves c-Met and EGFR signaling pathways in triple negative breast cancer cells. *PloS one* **8**(6): e65113.

Mehta RR, Katta H, Kalra A, Patel R, Gupta A, Alimirah F, Murillo G, Peng X, Unni A, Muzzio M and Mehta RG (2013b) Efficacy and mechanism of action of Deguelin in suppressing metastasis of 4T1 cells. *Clinical & experimental metastasis*.

Minet E, Mottet D, Michel G, Roland I, Raes M, Remacle J and Michiels C (1999) Hypoxia-induced activation of HIF-1: role of HIF-1alpha-Hsp90 interaction. *FEBS letters* **460**(2): 251-256.

Murillo G, Peng X, Torres KE and Mehta RG (2009) Deguelin inhibits growth of breast cancer cells by modulating the expression of key members of the Wnt signaling pathway. *Cancer prevention research* **2**(11): 942-950.

Oh SH, Woo JK, Jin Q, Kang HJ, Jeong JW, Kim KW, Hong WK and Lee HY (2008) Identification of novel antiangiogenic anticancer activities of deguelin targeting hypoxia-inducible factor-1 alpha. *International journal of cancer Journal international du cancer* **122**(1): 5-14.

Oh SH, Woo JK, Yazici YD, Myers JN, Kim WY, Jin Q, Hong SS, Park HJ, Suh YG, Kim KW, Hong WK and Lee HY (2007) Structural basis for depletion of heat shock protein 90 client proteins by deguelin. *Journal of the National Cancer Institute* **99**(12): 949-961.

Ramalingam S and Belani CP (2004) Paclitaxel for non-small cell lung cancer. *Expert opinion*

on pharmacotherapy **5**(8): 1771-1780.

Ratzke C, Mickler M, Hellenkamp B, Buchner J and Hugel T (2010) Dynamics of heat shock protein 90 C-terminal dimerization is an important part of its conformational cycle. *Proceedings of the National Academy of Sciences of the United States of America* **107**(37): 16101-16106.

Sawai A, Chandarlapaty S, Greulich H, Gonen M, Ye Q, Arteaga CL, Sellers W, Rosen N and Solit DB (2008) Inhibition of Hsp90 down-regulates mutant epidermal growth factor receptor (EGFR) expression and sensitizes EGFR mutant tumors to paclitaxel. *Cancer research* **68**(2): 589-596.

Sgobba M, Degliesposti G, Ferrari AM and Rastelli G (2008) Structural models and binding site prediction of the C-terminal domain of human Hsp90: a new target for anticancer drugs. *Chemical biology & drug design* **71**(5): 420-433.

Sharma SV, Bell DW, Settleman J and Haber DA (2007) Epidermal growth factor receptor mutations in lung cancer. *Nature reviews Cancer* **7**(3): 169-181.

Shimamura T and Shapiro GI (2008) Heat shock protein 90 inhibition in lung cancer. *Journal of thoracic oncology : official publication of the International Association for the Study of Lung Cancer* **3**(6 Suppl 2): S152-159.

Siegel R, Naishadham D and Jemal A (2013) Cancer statistics, 2013. *CA: a cancer journal for clinicians* **63**(1): 11-30.

Solar P, Horvath V, Kleban J, Koval J, Solarova Z, Kozubik A and Fedorocko P (2007) Hsp90 inhibitor geldanamycin increases the sensitivity of resistant ovarian adenocarcinoma cell line A2780cis to cisplatin. *Neoplasma* **54**(2): 127-130.

Soti C, Racz A and Csermely P (2002) A Nucleotide-dependent molecular switch controls ATP binding at the C-terminal domain of Hsp90. N-terminal nucleotide binding unmasks a C-terminal binding pocket. *The Journal of biological chemistry* **277**(9): 7066-7075.

Suh YA, Kim JH, Sung MA, Boo HJ, Yun HJ, Lee SH, Lee HJ, Min HY, Suh YG, Kim KW and

Lee HY (2013) A novel antitumor activity of deguelin targeting the insulin-like growth factor (IGF) receptor pathway via up-regulation of IGF-binding protein-3 expression in breast cancer. *Cancer letters* **332**(1): 102-109.

Tan C, de Noronha RG, Roecker AJ, Pyrzynska B, Khwaja F, Zhang Z, Zhang H, Teng Q, Nicholson AC, Giannakakou P, Zhou W, Olson JJ, Pereira MM, Nicolaou KC and Van Meir EG (2005) Identification of a novel small-molecule inhibitor of the hypoxia-inducible factor 1 pathway. *Cancer research* **65**(2): 605-612.

Thamilselvan V, Menon M and Thamilselvan S (2011) Anticancer efficacy of deguelin in human prostate cancer cells targeting glycogen synthase kinase-3 beta/beta-catenin pathway. *International journal of cancer Journal international du cancer* **129**(12): 2916-2927.

Trepel J, Mollapour M, Giaccone G and Neckers L (2010) Targeting the dynamic HSP90 complex in cancer. *Nature reviews Cancer* **10**(8): 537-549.

Wainberg ZA, Anghel A, Rogers AM, Desai AJ, Kalous O, Conklin D, Ayala R, O'Brien NA, Quadt C, Akimov M, Slamon DJ and Finn RS (2013) Inhibition of HSP90 with AUY922 induces synergy in HER2-amplified trastuzumab-resistant breast and gastric cancer. *Molecular cancer therapeutics* **12**(4): 509-519.

Whitesell L and Lindquist SL (2005) HSP90 and the chaperoning of cancer. *Nature reviews Cancer* **5**(10): 761-772.

Woo JK, Choi DS, Tran HT, Gilbert BE, Hong WK and Lee HY (2009) Liposomal encapsulation of deguelin: evidence for enhanced antitumor activity in tobacco carcinogen-induced and oncogenic K-ras-induced lung tumorigenesis. *Cancer prevention research* **2**(4): 361-369.

Zhang T, Hamza A, Cao X, Wang B, Yu S, Zhan CG and Sun D (2008) A novel Hsp90 inhibitor to disrupt Hsp90/Cdc37 complex against pancreatic cancer cells. *Molecular cancer therapeutics* **7**(1): 162-170.

Molecular Pharmacology Fast Forward. Published on May 14, 2015 as DOI: 10.1124/mol.114.096883
This article has not been copyedited and formatted. The final version may differ from this version.

Foot notes

Financial support: This work was supported by grants from the National Research Foundation of Korea (NRF), the Ministry of Science, ICT & Future Planning (MSIP), Republic of Korea [Nos. NRF-2011-0017639, NRF-2011-0019400, and NRF-2011-0030001].

Molecular Pharmacology Fast Forward. Published on May 14, 2015 as DOI: 10.1124/mol.114.096883
This article has not been copyedited and formatted. The final version may differ from this version.

Figure Legends

Figure 1. Minimal toxic effect of L80 in normal cells compared to deguelin

(A) Chemical structure of deguelin and L80. (B) Blood-Brain-Barrier permeability assay was conducted by using the PAMPA Explorer kit (*p*ION Inc.) Progesteron, and theophylline were used as positive, and negative control. (Pro: progesterone, Theo: theophylline, Deg: deguelin) (C-E) Mouse hppocampal (HT-22), Human umbilical vein endothelial (HUVEC), retinal pigment epithelial (RPE), and normal immortalized lung epithelial (HBEC and BEAS-2B) cells were treated with increasing concentrations of L80 or deguelin for 3 days. Values represent mean ± SD of experiments conducted in triplicate. **p* < 0.05, ***p* < 0.01, and ****p* < 0.001 by one-way analysis of variance (ANOVA) or Student's t-test compared with control group.

Figure 2. Inhibitory effects of L80 on the proliferation and colony formation of human lung cancer cells. (A-B) H1299, A549, H460, and H226B cells; paclitaxel-resistant lung cancer cells (H460/R and H226B/R); and were treated with increasing concentrations of L80 or deguelin for 3 days. Cell viability was determined by the MTT assay. (E) H1299, A549, H460, H460/R, H226B, and H226B/R cells were seeded onto 6-well plates at a density of 300 cells/well and then treated with L80 (0, 0.1, 1, and 10 μM). After two weeks, colonies were stained with crystal violet and counted. (F) The anchorage-independent growth of cells treated with increasing concentrations of L80 was determined by soft agar colony formation assay. All values represent mean ± SD of experiments conducted in triplicate. **p* < 0.05, ***p* < 0.01, and ****p* < 0.001 by one-way analysis of variance (ANOVA) compared with control group.

Figure 3. Induction of apoptosis by treatment with L80. (A) Cells were treated with L80 for 24 h. The distribution of cells in each phase of the cell cycle was analyzed by flow

Molecular Pharmacology Fast Forward. Published on May 14, 2015 as DOI: 10.1124/mol.114.096883
This article has not been copyedited and formatted. The final version may differ from this version.

cytometry. (B) The expression level of cleaved PARP after treatment with L80 in H1299 and H460/R cells was analyzed by Western blot analysis.

Figure 4. L80 exerts its antiangiogenic potential through inhibiting the stability and transcriptional activity of HIF-1α. (A) The HIF-1α expression level in the indicated NSCLC cells were treated with increasing concentrations of L80 under hypoxia condition was analyzed by Western blot analysis. (B) The indicated NSCLC cells were co-transfected with pGL3-basic or pGL3-HRE-Luc and pRL-TK-Luc. After treatment with L80 under hypoxia condition, luciferase activity was monitored as described in the Materials and Methods section. Values represent mean ± SD of experiments conducted in triplicate. *$p < 0.05$ by Student's t-test compared with control group. (C, D) The indicated NSCLC cells treated with increasing concentrations of L80 (C) or H1299 treated with 1 μM of deguelin or L80 (D) were subjected to RT-PCR, and Western blot analysis for the mRNA and protein expression of VEGF and IGF2. (E) HUVECs were treated with CM obtained from H1299 cells treated with increasing concentrations of L80 and incubated under hypoxic conditions. The morphological changes of HUVECs were imaged and scored. Values represent mean ± SD of experiments conducted in triplicate. *$p < 0.05$, ***$p < 0.001$ by one-way analysis of variance (ANOVA) compared with control group.

Figure 5. Inhibition of migration and invasion of lung cancer by treatment with L80. H1299, H226B, and H226B/R cells were seeded onto 96-well plates and incubated for 12h to evaluate proliferation effects by MTT assay (A). These cells also were seeded onto Transwells coated with either gelatin only (B) or gelatin and matrigel (C). After incubation for 18-19h, the migratory or invaded cells on the bottom of the membrane were stained and counted. All values represent mean ± SD of experiments conducted in triplicate. *$p < 0.05$, **$p < 0.01$, and ***$p < 0.001$ by Student's t-test compared with control group.

Molecular Pharmacology Fast Forward. Published on May 14, 2015 as DOI: 10.1124/mol.114.096883
This article has not been copyedited and formatted. The final version may differ from this version.

Figure 6. The antitumor effect of L80 in a tumor xenograft model. (A) H1299 cells were inoculated into the right flank of NOD/SCID mice. Mice harboring H1299 xenograft tumors were treated with vehicle or L80 for 3 weeks. The tumor sizes were monitored every day and were analyzed by one-way ANOVA compared with control group (0mg/kg). (B and C) The expression levels of cleaved caspase-3 and CD31 in xenograft tumors were analyzed by immunohistochemistry.

Figure 7. Downregulation of Hsp90 function by treatment with L80. (A) H1299 cells were treated with L80 under hypoxic conditions. Total cell lysates were prepared and immunoprecipitated with anti-HIF-1α antibodies. The interaction between HIF-1α and Hsp90 was analyzed by Western blot analysis. (B) H1299 lysates interacted with histidine-tagged recombinant HIF-1α in the presence or absence of L80. After pull-down with Ni-NTA agarose beads, the amount of Hsp90 bound to the recombinant HIF-1α was determined by Western blot analysis. (C) The expression levels of ErbB2 and Akt in the indiated NSCLC cells treated with increasing concentrations of L80 were analyzed by Western blot analysis. (D) Recombinant Hsp90 proteins containing the FL protein or the NM, M, and C domains interacted with ATP-agarose in the presence or absence of L80. The protein level bound to the ATP-agarose beads was determined by Western blot analysis. (E-G) Structural analysis of the binding of L80 to the C-terminal ATP binding pocket of Hsp90. (E) Docking study of ATP and L80 in the C-terminal ATP-binding pocket of hHsp90 homodimer. (F and G) Docking pose of L80 with the C-terminal hHsp90.

Molecular Pharmacology Fast Forward. Published on May 14, 2015 as DOI: 10.1124/mol.114.096883
This article has not been copyedited and formatted. The final version may differ from this version.

Figure 1

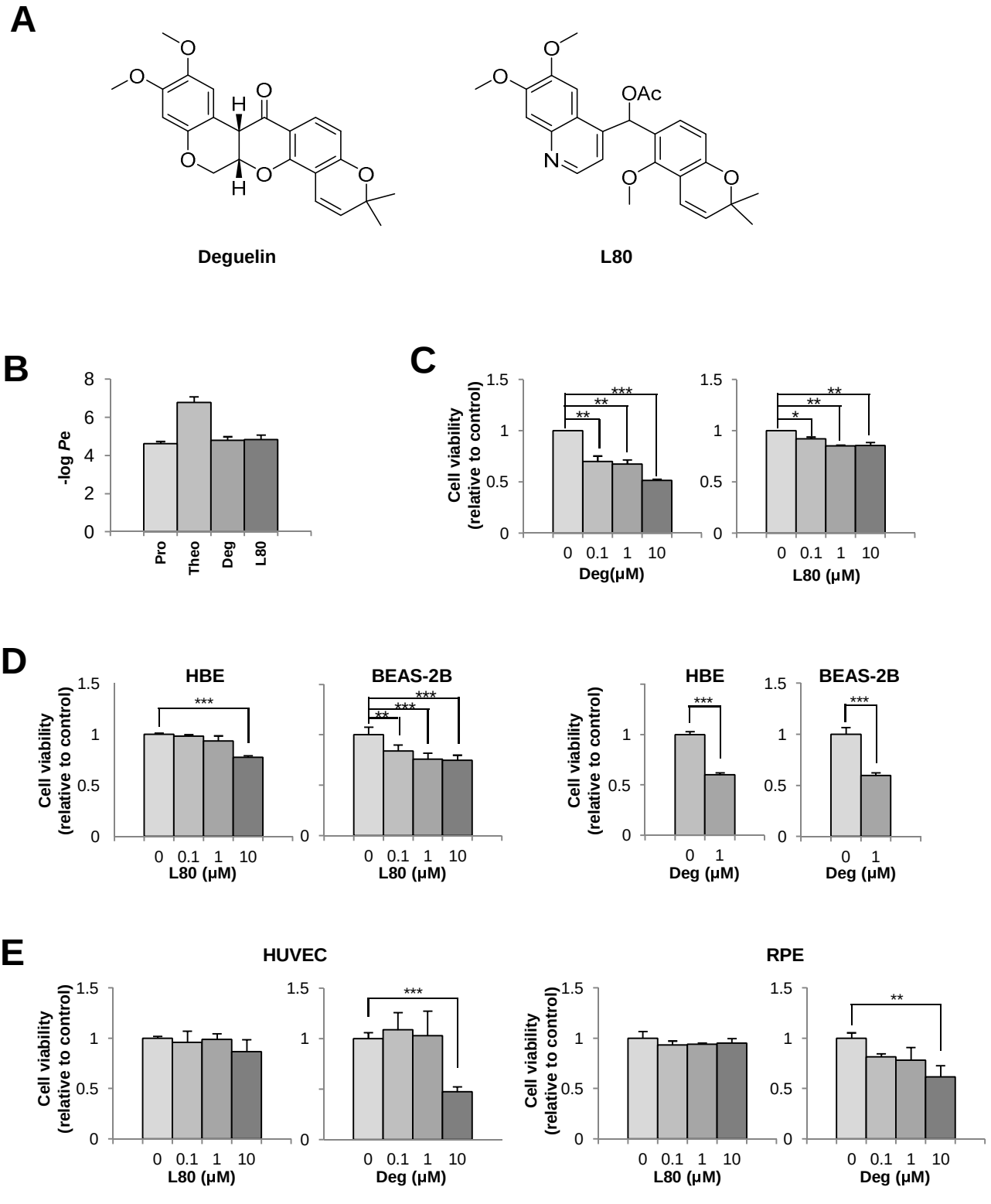

Molecular Pharmacology Fast Forward. Published on May 14, 2015 as DOI: 10.1124/mol.114.096883
This article has not been copyedited and formatted. The final version may differ from this version.

Figure 2

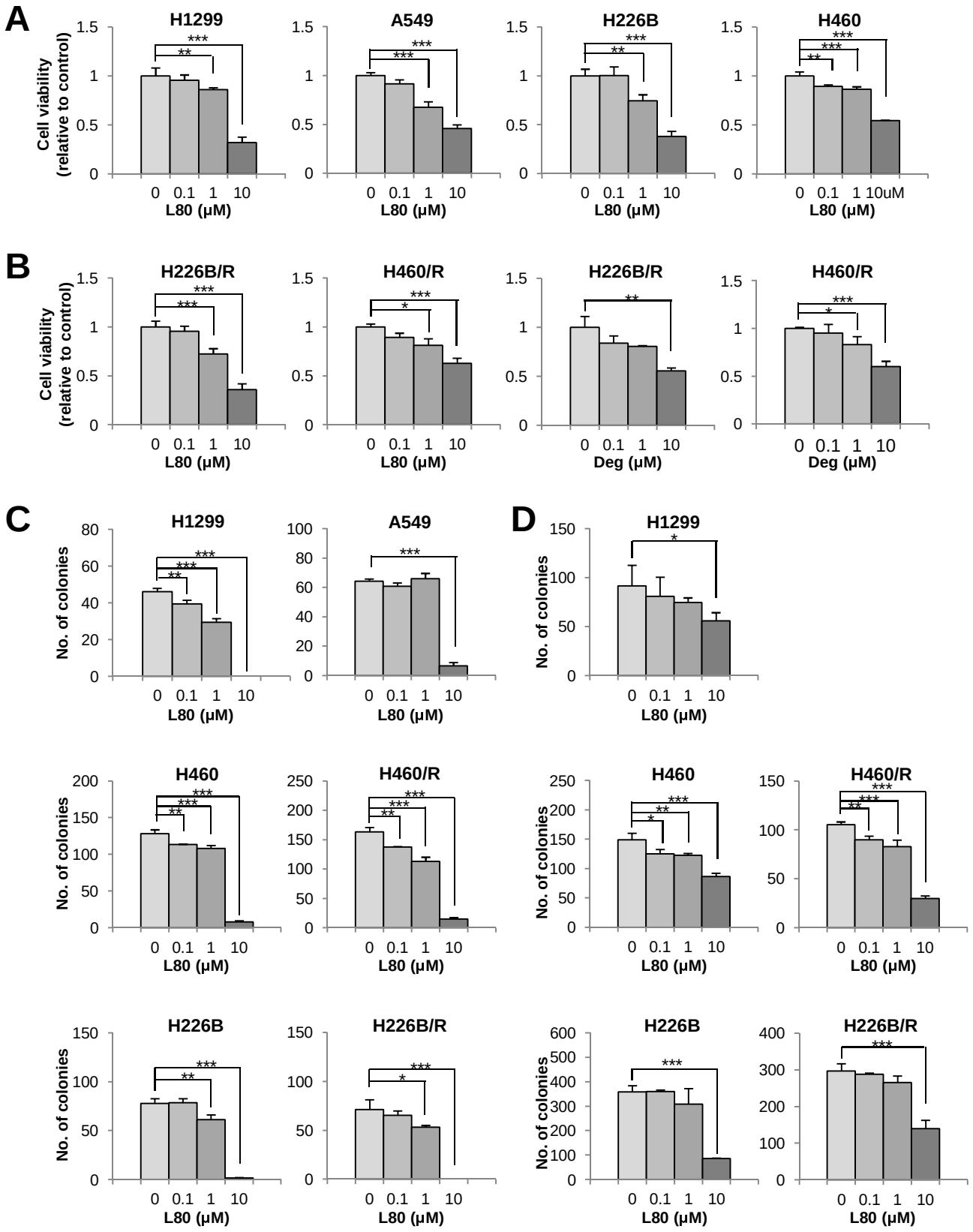

Molecular Pharmacology Fast Forward. Published on May 14, 2015 as DOI: 10.1124/mol.114.096883
This article has not been copyedited and formatted. The final version may differ from this version.

Figure 3

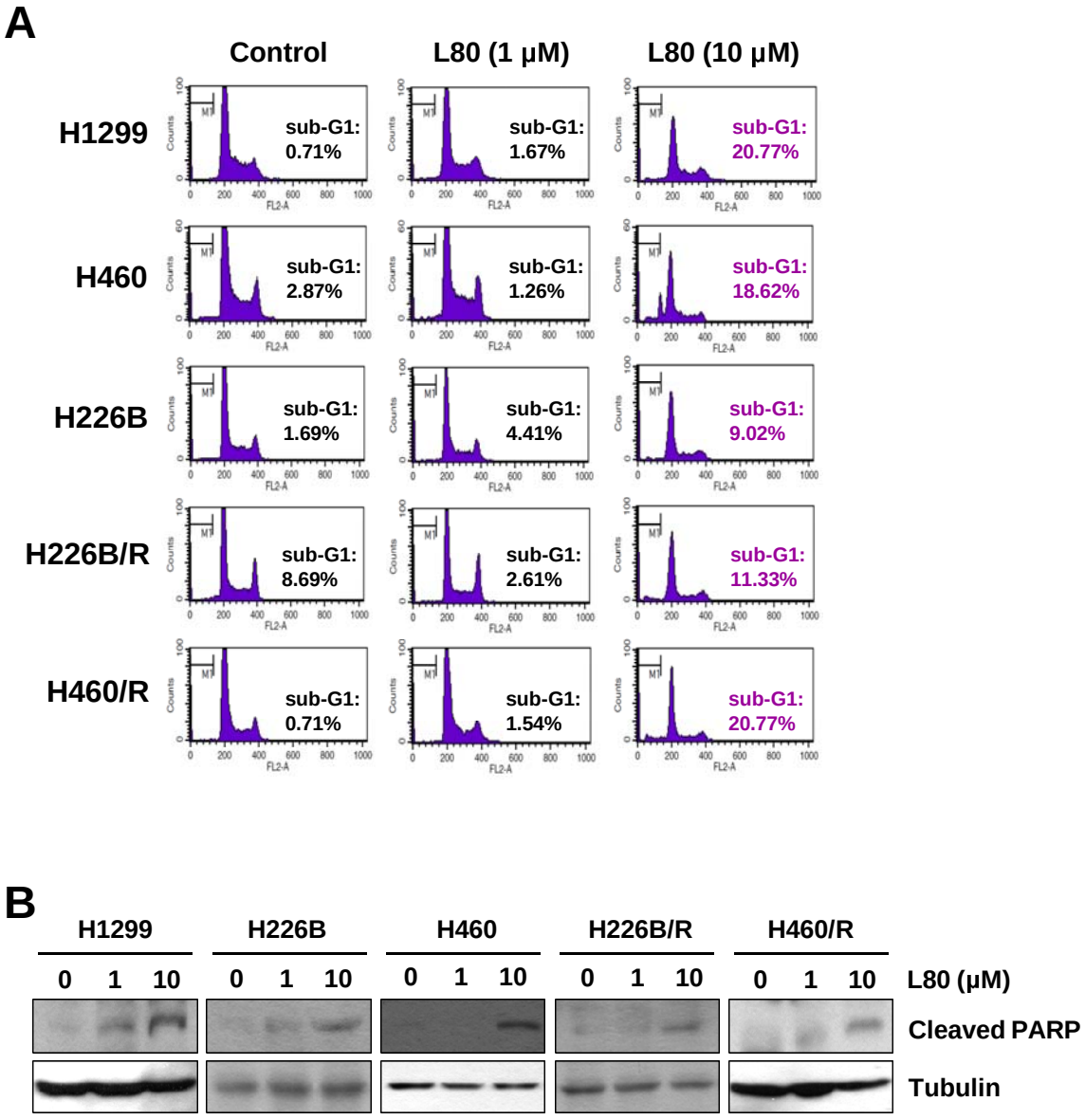

Molecular Pharmacology Fast Forward. Published on May 14, 2015 as DOI: 10.1124/mol.114.096883
This article has not been copyedited and formatted. The final version may differ from this version.

Figure 4

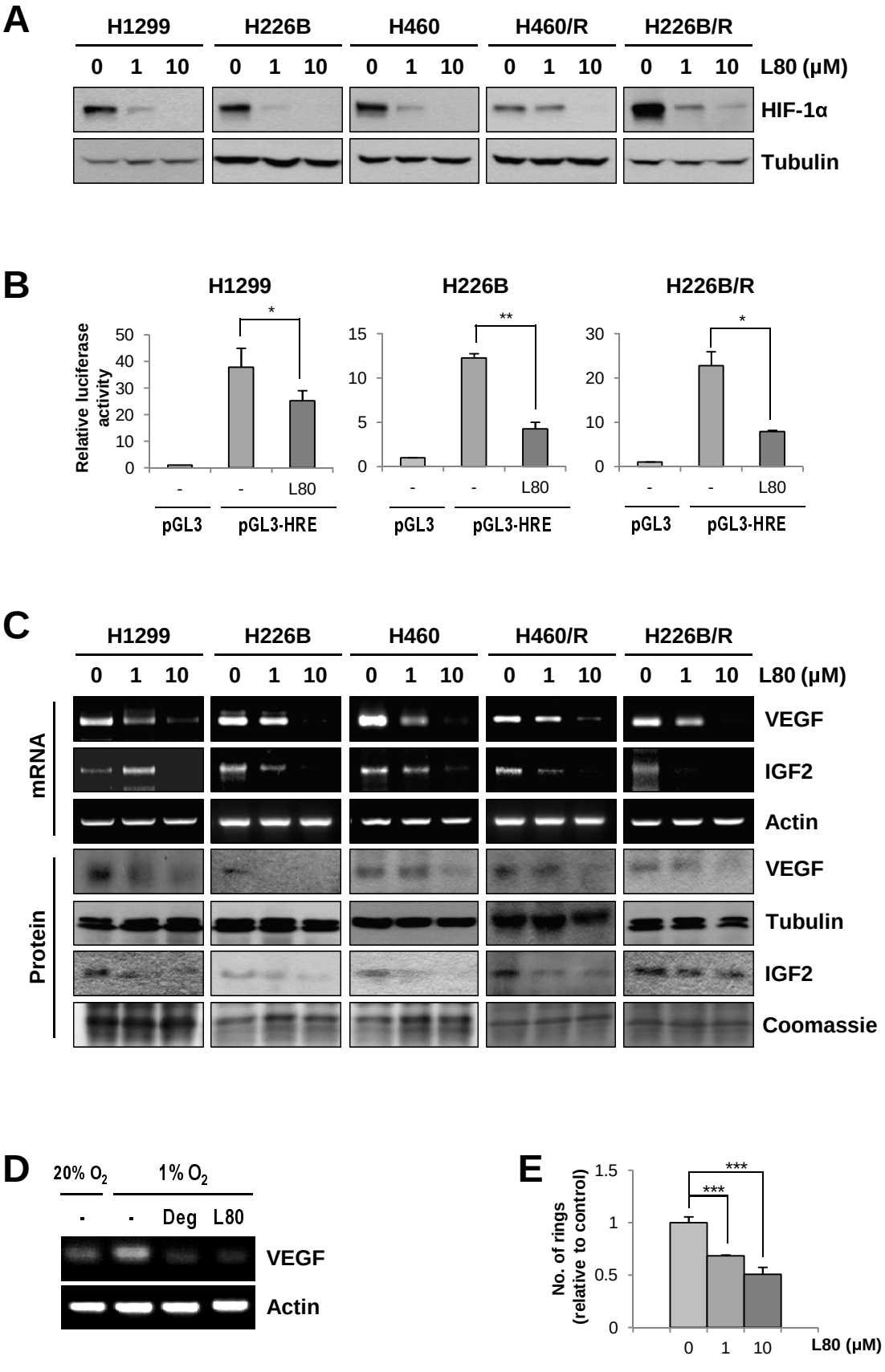

Molecular Pharmacology Fast Forward. Published on May 14, 2015 as DOI: 10.1124/mol.114.096883
This article has not been copyedited and formatted. The final version may differ from this version.

Figure 5

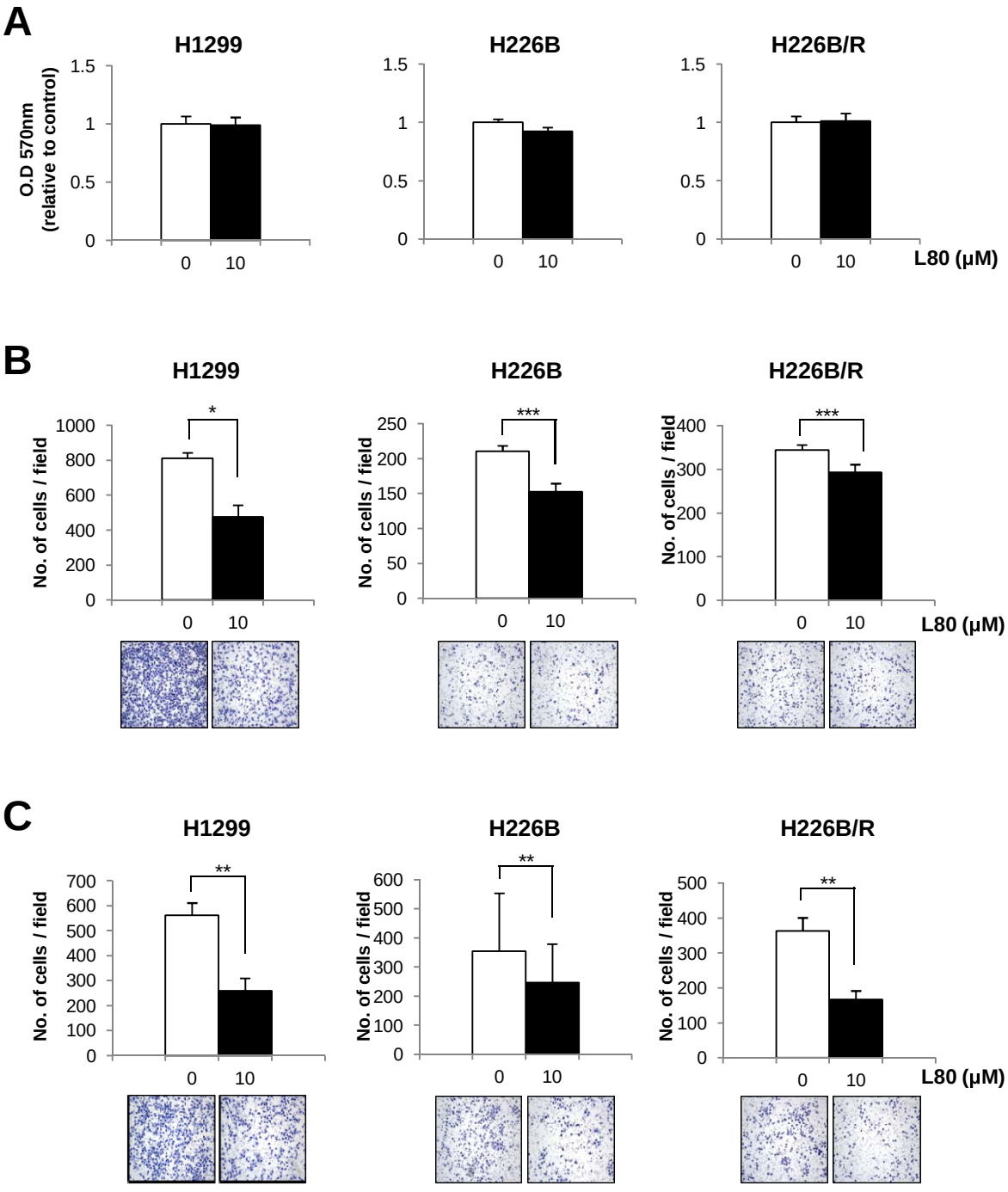

Molecular Pharmacology Fast Forward. Published on May 14, 2015 as DOI: 10.1124/mol.114.096883
This article has not been copyedited and formatted. The final version may differ from this version.

Figure 6

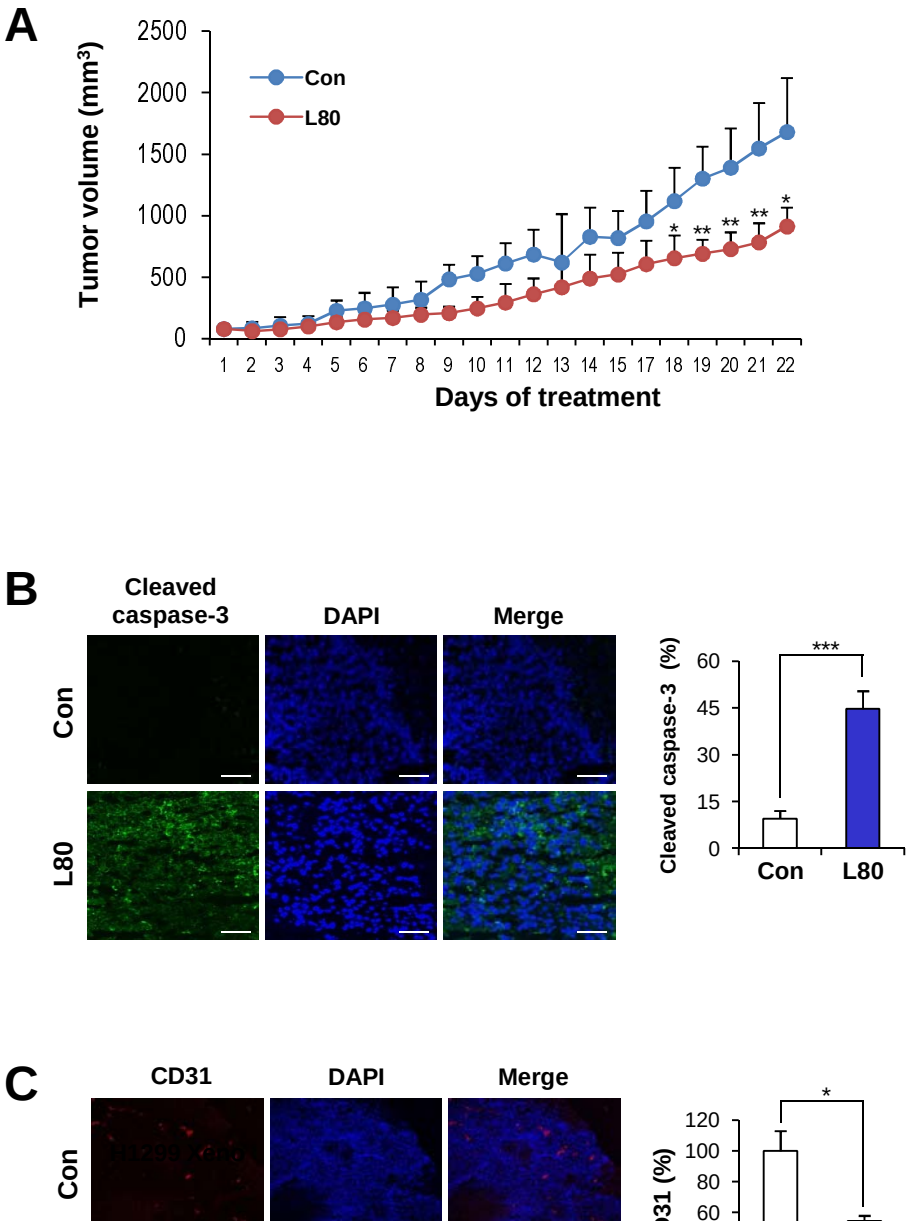

Molecular Pharmacology Fast Forward. Published on May 14, 2015 as DOI: 10.1124/mol.114.096883
This article has not been copyedited and formatted. The final version may differ from this version.

Figure 7

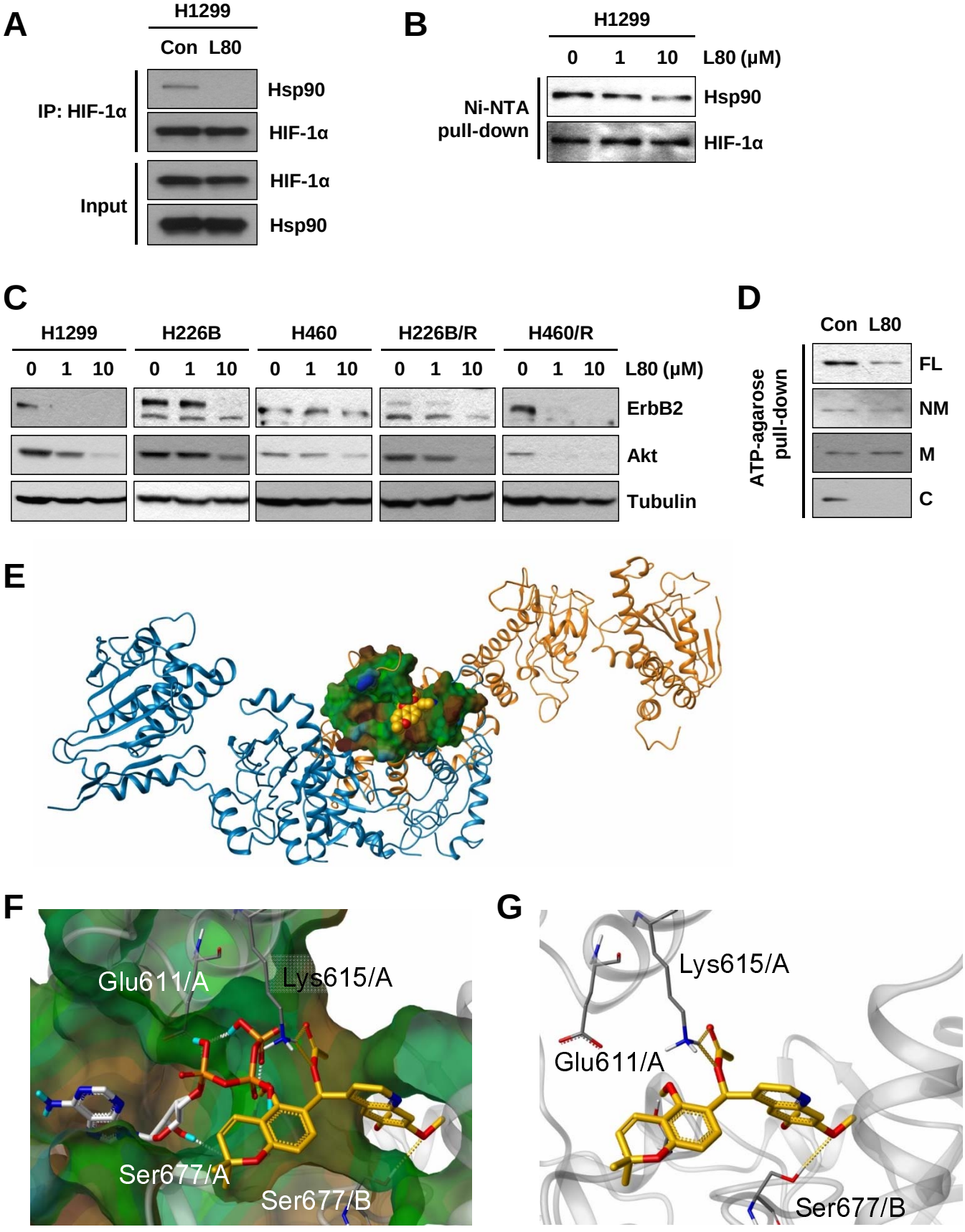

Supplemental Tables and Figures
MOL #96883

Synthesis and Evaluation of a Novel Deguelin Derivative, L80, which Disrupts ATP Binding to the C-terminal Domain of Heat Shock Protein 90

Su-Chan Lee, Hye-Young Min, Hoon Choi, Ho Shin Kim, Kyong-Cheol Kim, So-Jung Park, Myung A Sung, Ji Hae Seo, Hyun-Ju Park, Young-Ger Suh, Kyu-Won Kim, Jeewoo Lee, Ho-Young Lee

College of Pharmacy and Research Institute of Pharmaceutical Sciences, Seoul National University, Seoul 151-742, Republic of Korea (S.C.L., H.Y.M., H.C., H.S.K., K.C.K., M.A.S., J.H.S., Y.G.S., K.W.K., J.L., H.Y.L.)
School of Pharmacy, Sungkyunkwan University, Suwon 440-746, Korea (S.J.P., H.J.P.)

Table S1. BBB permeability of deguelin, L80, progesteron, and theophylline as determined by the Parallel Artificial Membrane Permeability assay.

Compound	-log *Pe**	CNS+/- prediction
Degueline	4.78±0.20	+
L80	4.82±0.25	+
Progesteron†	4.62±0.11	+
Theophylline†	6.77±0.30	-

*Average −log *P*e values were calculated by the PAMPA Explorer software v. 3.5.
† Progesteron, and theophylline were selected for comparison based on their known CNS activity

Table S2. Histology and genetic background of used cell lines

	EGFR	K-Ras	p53	PTEN	PI3KCA	LKB1	B-Raf
A549	WT	Mut	WT	WT	WT	Mut	WT
H226B	WT	WT	WT	U	WT	WT	WT
H1299	WT	WT	Nu	Nu	WT	WT	WT
H460	WT	Mut	WT	WT	Mut	Mut	WT

* WT: wild type Mut: mutnat type Nu: null U: unknown

Supplemental Figure Legends

Figure S1. Toxicity of L80 compared to deguelin (A) Blood-Brain-Barrier permeability assay was conducted by using the PAMPA Explorer kit (*p*ION Inc.) Progesteron, and theophylline were used as positive, and negative control. (Pro: progesterone, Theo: theophylline, Deg: deguelin) (B-D) Mouse hppocampal cell (HT-22 cell), Human umbilical vein endothelial (HUVEC), retinal pigment epithelial (RPE), and normal immortalized lung epithelial cells (HBEC and BEAS-2B) were treated with increasing concentrations of L80 or deguelin for 3 days. Values represent mean ± SD of experiments conducted in triplicate. *$p < 0.05$, **$p < 0.01$, and ***$p < 0.001$ by one-way analysis of variance (ANOVA) or Student's t-test compared with control group.

Figure S2. Inhibitory effects of L80 on the proliferation and colony formation of human lung cancer cells. (A) H1299, A549, H460, and H226B cells; paclitaxel-resistant lung cancer cells (H460/R and H226B/R); and were treated with increasing concentrations of L80 or deguelin for 3 days. Cell viability was determined by the MTT assay. (B) H1299, A549, H460, H460/R, H226B, and H226B/R cells were seeded onto 6-well plates at a density of 300 cells/well and then treated with L80 (0, 0.1, 1, and 10 μM). After two weeks, colonies were stained with crystal violet and counted. (C) The anchorage-independent growth of cells treated with increasing concentrations of L80 was determined by soft agar colony formation assay. All values represent mean ± SD of experiments conducted in triplicate. *$p < 0.05$, **$p < 0.01$, and ***$p < 0.001$ by one-way analysis of variance (ANOVA) compared with control group.

Figure S3. Induction of apoptosis by treatment with L80. (A) Cells were treated with L80 for 24 h. The distribution of cells in each phase of the cell cycle was analyzed by flow cytometry.

Figure S4. L80 exerts its antiangiogenic potential through inhibiting the stability and transcriptional activity of HIF-1α. (A) The HIF-1α expression level in the indicated NSCLC cells were treated with increasing concentrations of L80 under hypoxia condition was analyzed by Western blot analysis. (B) The indicated NSCLC cells were co-transfected with pGL3-basic or pGL3-HRE-Luc and pRL-TK-Luc. After treatment with L80 under hypoxia condition, luciferase activity was monitored as described in the Materials and Methods section. Values represent mean ± SD of experiments conducted in triplicate. *$p < 0.05$ by Student's t-test compared with control group. (C, D) The indicated NSCLC cells treated with increasing concentrations of L80 (C) or H1299 treated with 1 μM of deguelin or L80 (D) were subjected to RT-PCR for the mRNA expression of VEGF and IGF2. (E) HUVECs were treated with CM obtained from H1299 cells treated with increasing concentrations of L80 and incubated under hypoxic conditions. The morphological changes of HUVECs were imaged and scored. Values represent mean ± SD of experiments conducted in triplicate. *$p < 0.05$, ***$p < 0.001$ by one-way analysis of variance (ANOVA) compared with control group (0μM of L80).

Figure S5. Inhibition of migration and invasion of lung cancer by treatment with L80. H1299, H226B, and H226B/R cells were seeded onto 96-well plates and incubated for 12h to evaluate proliferation effects by MTT assay (A). These cells also were seeded onto Transwells coated with either gelatin only (B) or gelatin and matrigel (C). After incubation for 18-19h, the migratory or invaded cells on the bottom of the membrane were stained and counted. All values represent mean ± SD of experiments conducted in triplicate. *$p < 0.05$, **$p < 0.01$, and ***$p < 0.001$ by Student′s *t*-test compared with control group.

Figure S6. The effect of L80 on body weight in a tumor xenograft model. H1299 cells were inoculated into the right flank of NOD/SCID mice. Mice harboring H1299 xenograft tumors were treated with vehicle or L80 for 3 weeks. The body weight were monitored on 1day, and 20days. Body weight was analyzed by one-way analysis of variance (ANOVA) compared with control group (0mg/kg).

Figure S7. Downregulation of Hsp90 function by treatment with L80. (A) H1299 cells were treated with L80 under hypoxic conditions. Total cell lysates were prepared and immunoprecipitated with anti-HIF-1α antibodies. The interaction between HIF-1α and Hsp90 was analyzed by Western blot analysis. (B) H1299 lysates interacted with histidine-tagged recombinant HIF-1α in the presence or absence of L80. After pull-down with Ni-NTA agarose beads, the amount of Hsp90 bound to the recombinant HIF-1α was determined by Western blot analysis. (C) The expression levels of ErbB2 and Akt in the indiated NSCLC cells treated with increasing concentrations of L80 were analyzed by Western blot analysis. (D) Recombinant Hsp90 proteins containing the FL protein or the NM, M, and C domains interacted with ATP-agarose in the presence or absence of L80. The protein level bound to the ATP-agarose beads was determined by Western blot analysis.

Figure S8. Full blots of cleaved parp in NSCLC cells. H1299, H226B,H460, H226B/R, and H460/R cells were seeded and treated with 0, 1, and 10 μM L80 for 24 h. Cell lysates were obtained by RIPA buffer and determined by Western blot analysis.

Figure S1

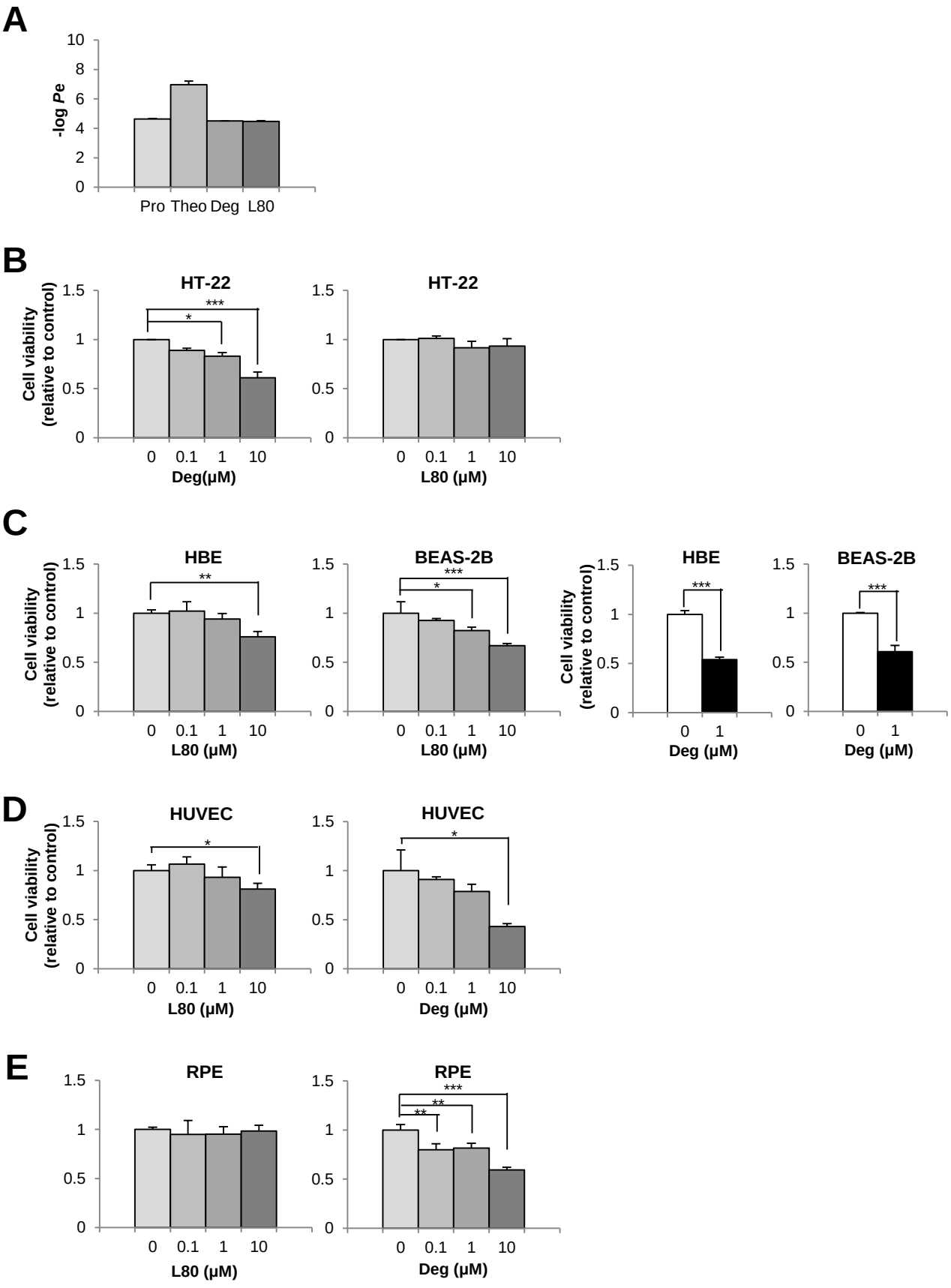
A
-log Pe
Pro Theo Deg L80
B
HT-22
HT-22
Cell viability (relative to control)
Deg(μM)
L80 (μM)
C
HBE
BEAS-2B
HBE
BEAS-2B
L80 (μM)
Deg (μM)
D
HUVEC
HUVEC
L80 (μM)
Deg (μM)
E
RPE
RPE
L80 (μM)
Deg (μM)

Figure S2

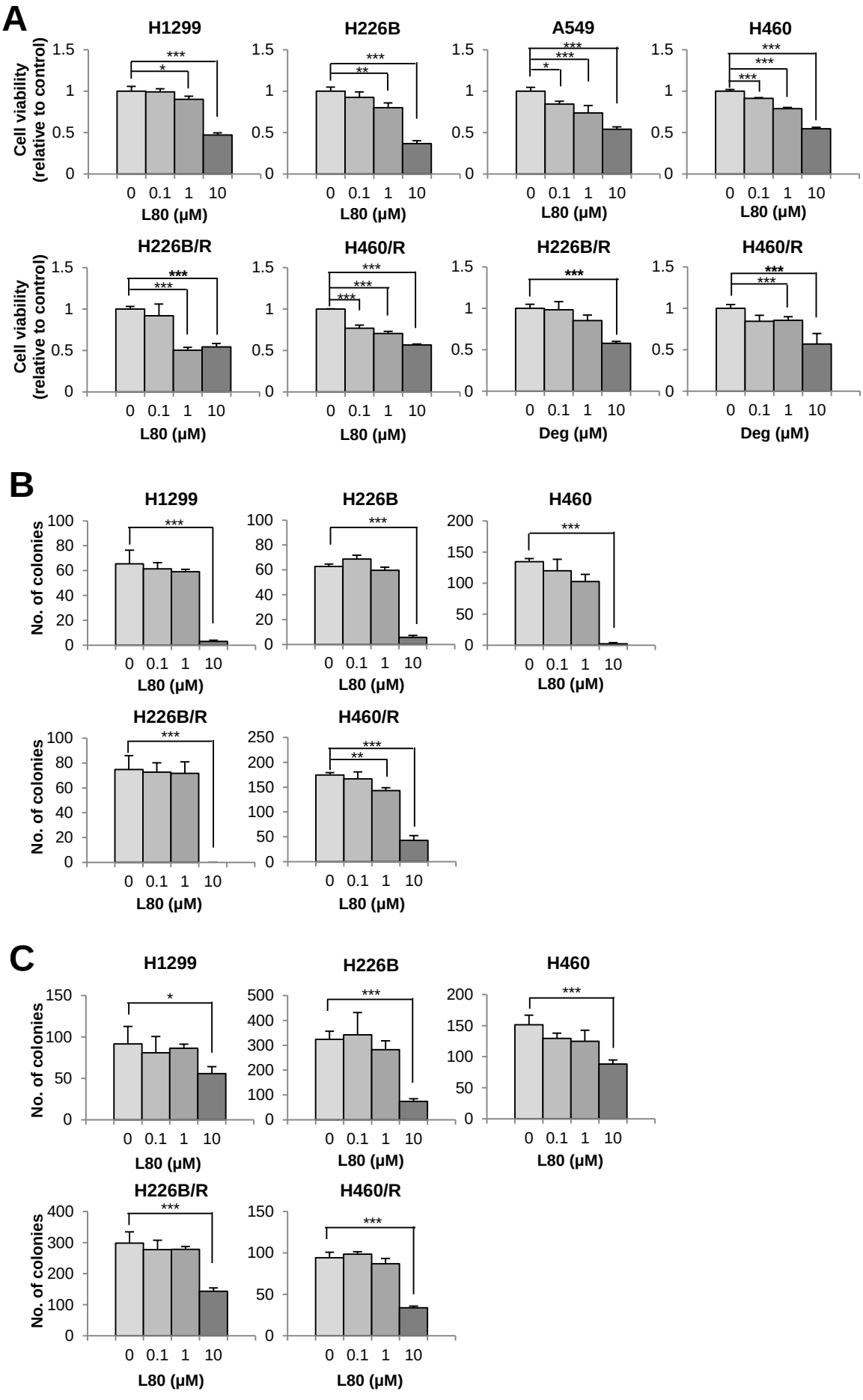
A
H1299
H226B
A549
H460
H226B/R
H460/R
Cell viability (relative to control)
L80 (μM)
Deg (μM)
B
No. of colonies
C

Figure S3

A

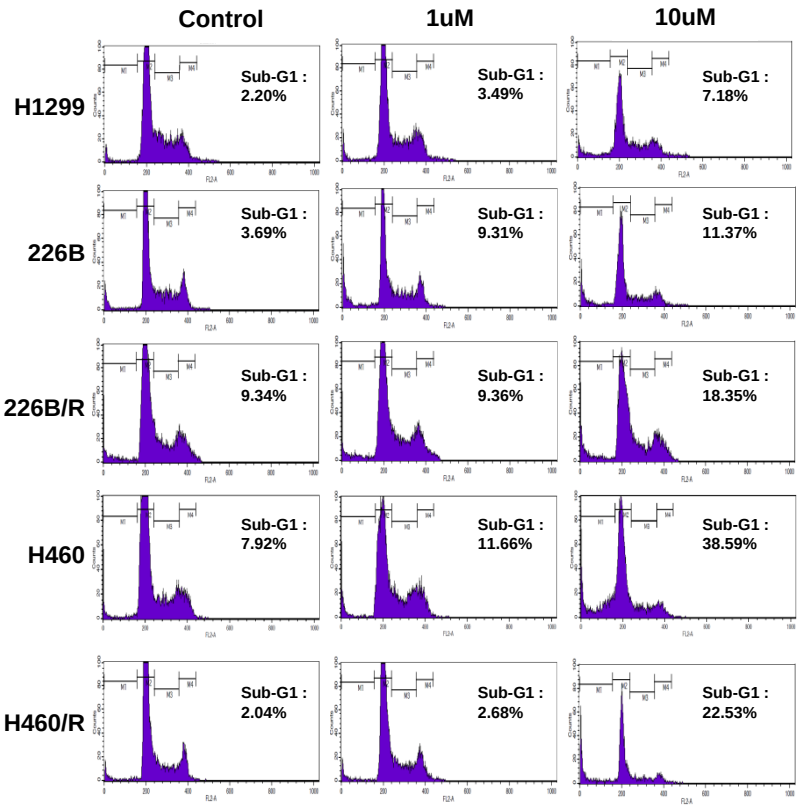
Control
1uM
10uM
H1299
Sub-G1 : 2.20%
Sub-G1 : 3.49%
Sub-G1 : 7.18%
226B
Sub-G1 : 3.69%
Sub-G1 : 9.31%
Sub-G1 : 11.37%
226B/R
Sub-G1 : 9.34%
Sub-G1 : 9.36%
Sub-G1 : 18.35%
H460
Sub-G1 : 7.92%
Sub-G1 : 11.66%
Sub-G1 : 38.59%
H460/R
Sub-G1 : 2.04%
Sub-G1 : 2.68%
Sub-G1 : 22.53%

Figure S4

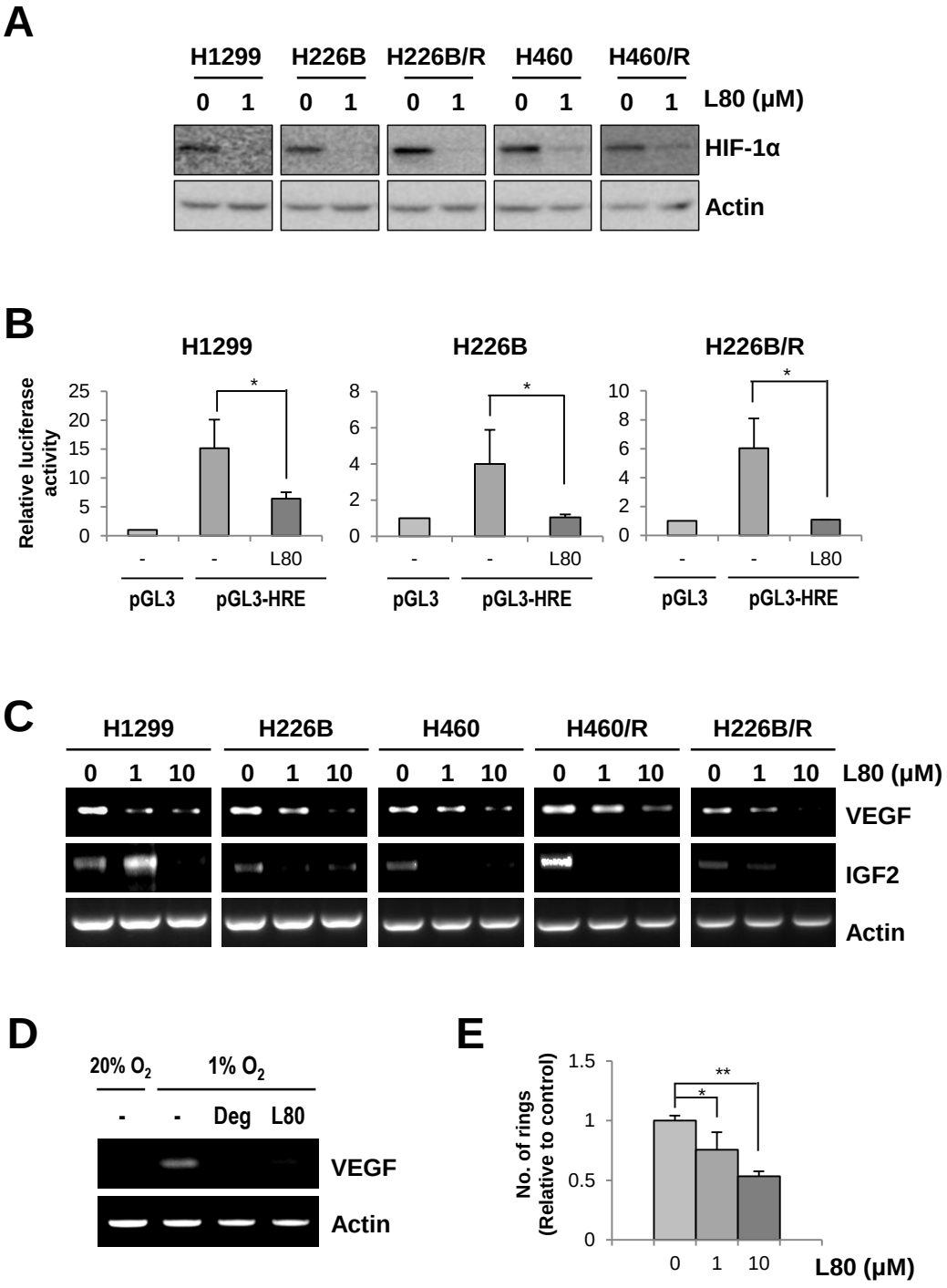
A
H1299
H226B
H226B/R
H460
H460/R
0 1 0 1 0 1 0 1 0 1
L80 (μM)
HIF-1α
Actin
B
H1299
H226B
H226B/R
Relative luciferase activity
25
20
15
10
5
0
8
6
4
2
0
10
8
6
4
2
0
*
- - L80
pGL3
pGL3-HRE
C
H1299
H226B
H460
H460/R
H226B/R
0 1 10 0 1 10 0 1 10 0 1 10 0 1 10
L80 (μM)
VEGF
IGF2
Actin
D
20% O2
1% O2
- - Deg L80
VEGF
Actin
E
No. of rings (Relative to control)
1.5
1
0.5
0
**
*
0 1 10
L80 (μM)

Figure S5

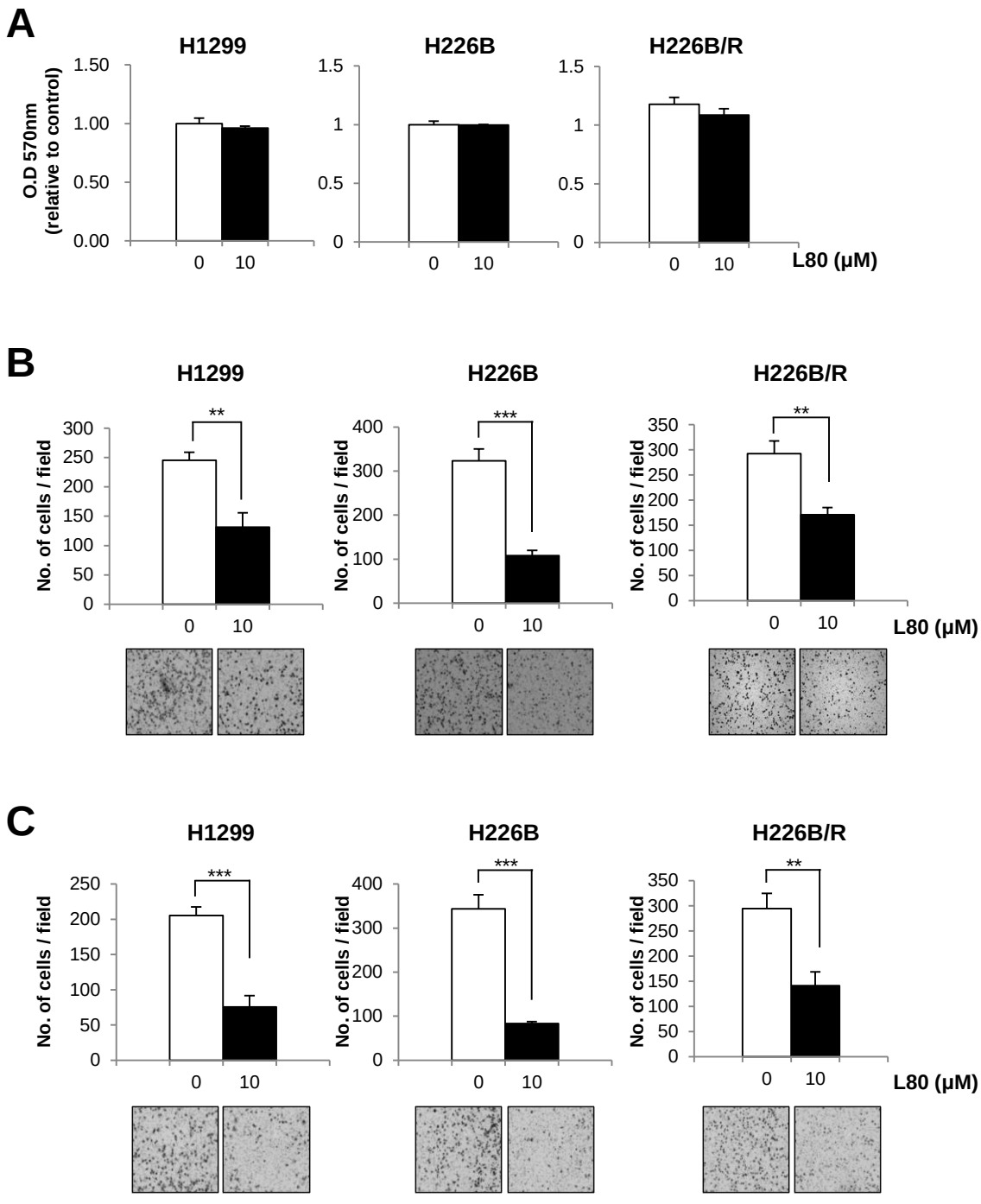
A
H1299
H226B
H226B/R
O.D 570nm
(relative to control)
1.50
1.00
0.50
0.00
1.5
1
0.5
0
0
10
L80 (μM)
B
H1299
H226B
H226B/R
No. of cells / field
**
***
**
300
250
200
150
100
50
0
400
350
0
10
L80 (μM)
C
H1299
H226B
H226B/R
No. of cells / field
***
***
**
250
200
150
100
50
0
400
350
300
0
10
L80 (μM)

Figure S6

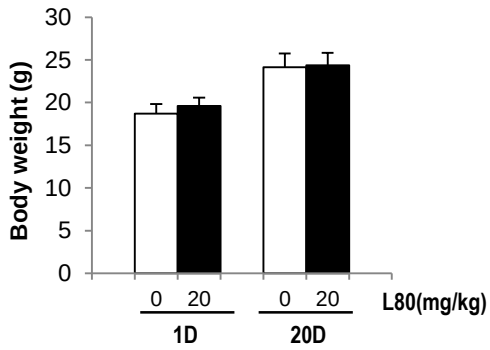

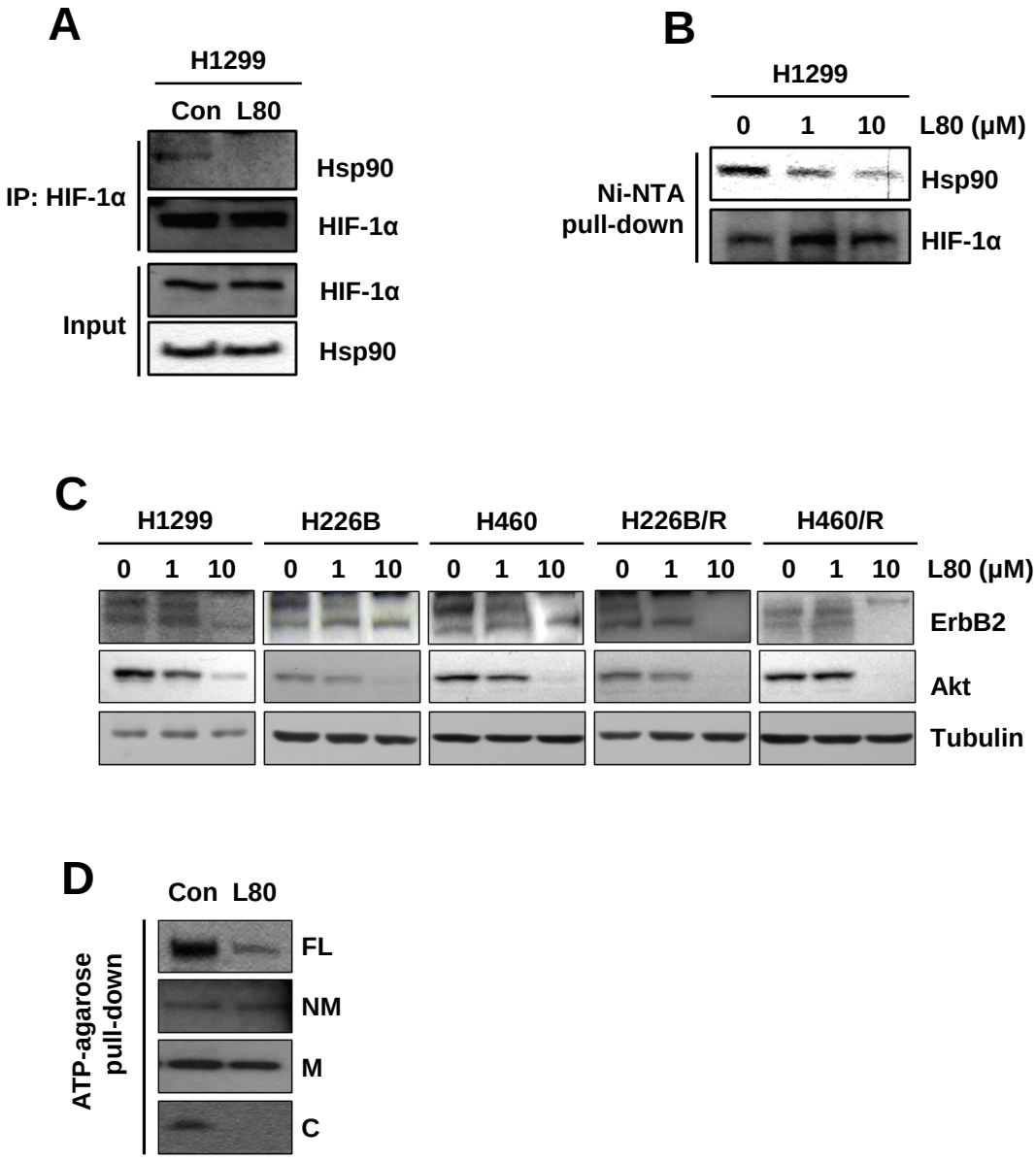
A
H1299
Con L80
IP: HIF-1α
Hsp90
HIF-1α
Input
HIF-1α
Hsp90
B
H1299
0 1 10 L80 (μM)
Ni-NTA pull-down
Hsp90
HIF-1α
C
H1299 H226B H460 H226B/R H460/R
0 1 10 0 1 10 0 1 10 0 1 10 0 1 10 L80 (μM)
ErbB2
Akt
Tubulin
D
Con L80
ATP-agarose pull-down
FL
NM
M
C

Figure S8

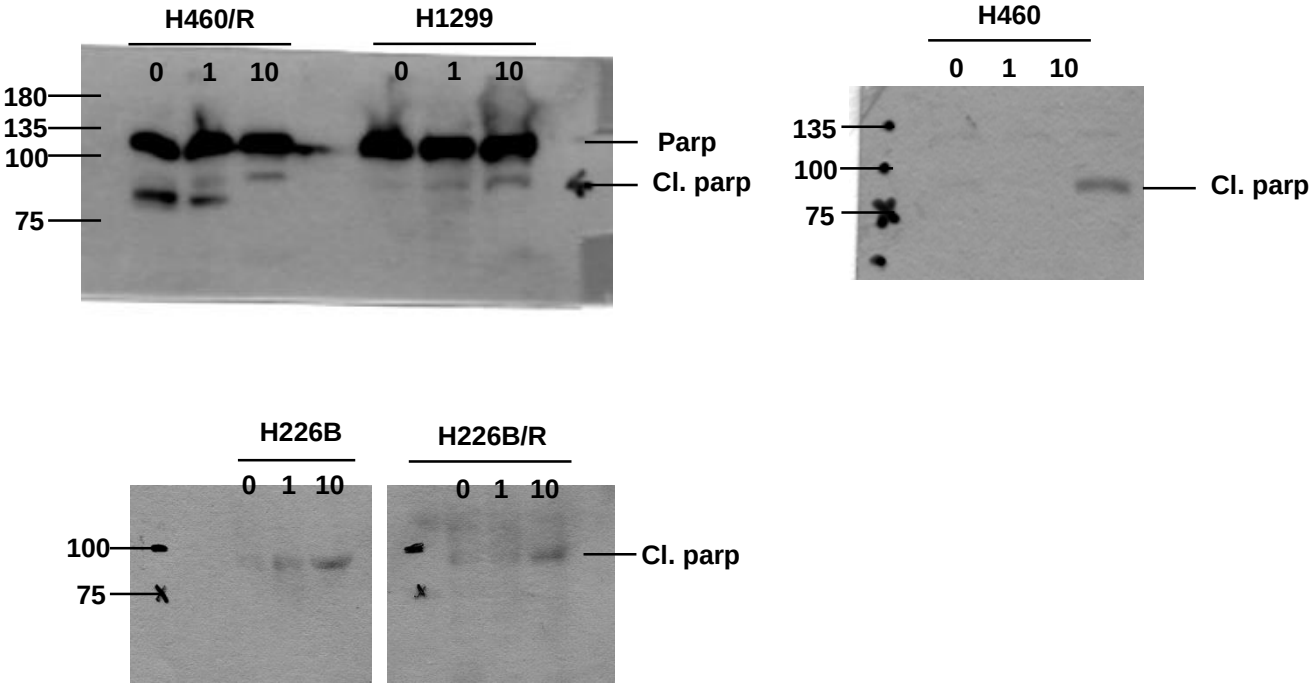
H460/R
H1299
0 1 10
0 1 10
180
135
100
75
Parp
Cl. parp
H460
0 1 10
135
100
75
Cl. parp
H226B
H226B/R
0 1 10
0 1 10
100
75
Cl. parp